

Department of Mechanical Engineering

**LIGHT AIR RECONNAISSANCE
PLATFORM**



In partial fulfillment to the requirements for the

Degree of Bachelor of Engineering

Session 2004/2005

National University of Singapore

Submitted by

CHUA SHYAN JIN, RONALD

U015714X

Abstract

The main objective of this project is to develop a proof of concept, autonomous flight platform. This project is an industrial collaboration with HQ Combat Engineers. The flight platform chosen for demonstrating autonomous navigation and surveillance is a non rigid airship, otherwise known as a blimp. A remote control blimp was purchased from Canada and the controls were extensively modified.

The key challenge in this project was the development of an in-house autonomous flight navigation and surveillance control system. It was a multidisciplinary objective, and required extensive knowledge of electronics, mechanical actuation and programming.

An electronics system for autonomous flight navigation and surveillance was designed and built in house. This system consists of the use of a microcontroller at its core, the PIC18F452, as well as other integrated circuits, such as the L293D, 74HC08, MAX232. 4 different Printed Circuit Boards (PCBs) were designed using software, the Protel Design System. These 4 boards were the Central Processing Unit (CPU) Board, the GPS receiver Board, the RS 232 Board and the Motor Drive Board. These PCBs were then fabricated.

The source code required for achieving autonomous flight navigation and surveillance was developed from scratch. Codes for the various functions, such as LED timing and control and reading GPS outputs from the receiver, were written in “C” programming language. These were integrated and used in the development of the main source code.

Experimental flight tests on the actual platform, an 8 foot long blimp, were carried out to verify the effectiveness of the control system, which had been developed in-house. The initial flight tests were observed to be unsatisfactory due to the controls that came with the blimp. The problem was analyzed using fundamentals of dynamics. A method was devised to solve this by using 2 thrust motors. The thrust motors were modified from dependant, on-off, single direction motors to independent, variable speed, bi-directional thrust motors. A proportional control was also developed. Implementation of this new method of control saw the completion of objectives of this project.

To accomplish further objectives, the wind force on the flight platform was investigated under various wind speeds. Experiments were also carried out to quantify the thrust forces provided by the propellers spinning in both the forward and reverse directions. The knowledge gathered from the 2 experiments was used to formulate an equation that defined the maximum operating conditions for a blimp of a given size.

Experiments to quantify the wind force and propeller thrust force were done and the results used to formulate an equation for the maximum operating condition of an airship.

A paper on this project, titled GPS System Design and Control Modeling, was also presented at the Aerospace Technology Seminar 2005 organized by the Republic of Singapore Air Force.



Acknowledgements

The author will like to thank his supervisor, Associate Professor Gerard Leng S. B., for his support, guidance, and counsel throughout the entire duration of this project. Furthermore, the author would like to thank his professor for having made possible the presentation at the ATS 2005.

The author will also like to thank the kind sponsors of this project, HQ SCE, for providing the funds without which this project wouldn't have been possible.

The author will specially like to thank his parents and his girlfriend, Ms Joan Huang, for their total support and for waking up in the wee hours of the morning to help him conduct his dawn flight tests, which saw the successful completion of this project.

The author would also like to thank the following people who have, in one way or another, made this project a success.

The Staff of Dynamics Lab, NUS

Mr. Low Yee Leong – Masters Student

Mr. Low Jun Hong – Fellow FYP Student

Mr. Neo Kok Yong – Dinkum Technologies

Mr. Jalin – PCB fabrication lab, NUS

Mr. Yee Choon Seng – Control Lab, NUS

Mr. Tan Tu Yii – Fellow FYP Student

CPT Edwin – HQ SCE Liaison Officer

Table of Contents

ABSTRACT	I
ACKNOWLEDGEMENTS	III
TABLE OF CONTENTS	IV
LIST OF FIGURES	IX
LIST OF SYMBOLS	XII
1. Introduction	1
1.1 Objectives	2
1.2 Organization of Thesis	3
1.3 Acknowledgement of Previous Project	4
2. Choice and Analysis of Platform	4
2.1 Comparison against other platforms	5
2.2 Autonomous Flight Control	6
3. Design of GPS Navigation System	7
3.1 Parameters of GPS Module	7
3.2 GPS Modules sourced	9
3.3 Analysis and choice of GPS module	10
4. Design and Fabrication of Electronic Hardware	11
4.1 Microcontroller Board	12
4.2 GPS Receiver Board	13
4.3 Motor Drive Board	14
4.4 RS-232 Interface Board	15
4.5 Electronic Compass	16

5. Modification of Mechanical Actuators	17
5.1 Rudder Motor Approach	18
5.2 A Better System – Bi-Directional Thrust Motors	19
5.3 Analysis and Choice of Approach	21
6. Development of Source Code	21
6.1 Choice of Programming Language	22
6.2 Function Development	23
6.2.1 Lighting LEDs with timing control	23
6.2.2 Serial Transmit and Receive	23
6.2.3 Servo Motor and DC Motor control	23
6.2.4 Variable DC Motor Speed and Direction Control	24
6.2.5 Bearing Reading from Electronic Compass	24
6.2.6 Reading GPS coordinate outputs	25
6.3 Overview of Source Code	25
6.4 Main Functions of Source Code	26
6.4.1 Authentication	26
6.4.2 Waypoint Input	26
6.4.3 Navigation	26
6.4.4 Stationary Surveillance	27
7. Surveillance System	28
7.1 Wireless Camera	28
7.2 Receiver Hardware and Software	29

8. Scaling up of System for Operational Deployment	29
8.1 Wind Force Determination	29
8.2 Thrust Force Determination	31
8.3 Weight Considerations	33
9. Design and Verification of Control System	34
9.1 Obtaining Transfer Function	35
9.2 Implementation of Proportional Yaw Control (During Navigation)	36
9.3 Implementation of Proportional Yaw Control (Stationary Surveillance)	37
9.4 Implementation of Proportional Thrust Control	38
10. System Development and Integration	38
10.1 Breadboard Development	39
10.2 Temporary Gondola Verification	39
10.3 Integrating into Actual Gondola	40
11. Flight Tests	42
12. Evaluation of Autonomous Airship Developed	45
13. Recommendations	46
14. Conclusion	47
References	50

Appendix 2.1 – Picture of Blimp and Control System	i
Appendix 3.1 – NMEA Field Definitions	ii
Appendix 3.2 – NMEA 0183 GPGGA Message Format	iv
Appendix 3.3 – Relative Weighing Factor Chart	v
Appendix 3.4 – GPS Modules Sourced	vi
Appendix 3.5 – Go/No Go & Weighted Property Index Chart	vii
Appendix 3.6 – Technical Drawing of Trimble Lassen GPS Receiver	viii
Appendix 3.7 – Technical Drawing of Trimble Magnetic Mount GPS Antenna	ix
Appendix 4.1 – Protel Design of CPU PCB	x
Appendix 4.2 – Components in CPU PCB	xi
Appendix 4.3 – Graph of Different Logic Formats	xii
Appendix 4.4 – Protel Design of GPS Receiver PCB	xiii
Appendix 4.5 – Components in GPS Receiver PCB	xiv
Appendix 4.6 – Protel Design of Motor Drive PCB	xv
Appendix 4.7 – Components in Motor Drive PCB	xvi
Appendix 4.8 – RS 232 Voltage Levels	xvii
Appendix 4.9 – Protel Design of RS 232 PCB	xvii
Appendix 4.10 – Components in RS 232 PCB	xix
Appendix 5.1 – Duty Cycle Concept	xx
Appendix 6.1 – Code for “Lighting LEDs with timing control”	xxi
Appendix 6.2 – Code for “Serial Transmit and Receive”	xxii
Appendix 6.3 – Code for “Servo and DC Motor Control”	xxiii
Appendix 6.4 – Code for “Variable DC Motor Speed and Direction Control”	xxv

Appendix 6.5 – Code for “Bearing Reading from electronic compass”	xxviii
Appendix 6.6 – Code for “Reading GPS coordinate outputs from GPS Receiver”	xxx
Appendix 6.7 – Source Code	xxxix
Appendix 7.1 – Resolution Capabilities of wireless camera system	xlvii
Appendix 8.1 – Graph of Wind Force Vs Wind Speed Sq (Head Wind)	xlviii
Appendix 8.2 – Derivation of C_D	xlix
Appendix 8.3 – Graph of Thrust Force in the Forward Direction Vs Duty Cycle	l
Appendix 8.4 – Graph of Thrust Force in the Reverse Direction Vs Duty Cycle	li
Appendix 8.5 – Derivation of Equation for Maximum Operating Conditions of Current Platform	lii
Appendix 8.6 – Derivation of General Equation For Maximum Operating Conditions	liii
Appendix 8.7 – Weight of Various Components (Remain the same)	liv
Appendix 8.8 – Weight of Various Components (Changes and Optional)	lv
Appendix 8.9 – Payloads and Weight Considerations of Different Sized Airships	lvi
Appendix 9.1 – Block Diagram of GPS Navigation Control Loop	lvii
Appendix 9.2 – Output Response of Plant to Step Input	lviii
Appendix 9.3 – Curve Fitting using Complex RF	lix
Appendix 9.4 – Derivation of Transfer Function of Plant	lxi
Appendix 9.5 – Graph of Duty Cycle Vs Bearing Error for Navigational Yaw Control	lxii
Appendix 9.6 – Graph of Duty Cycle Vs Bearing Error for Stationary Yaw Control	lxiii
Appendix 9.7 – Graph to Determine Rise Times	lxiv
Appendix 10.1 – Components in Unmodified Gondola	lxv
Appendix 10.2 – Components in Modified Gondola	lxvi

List of Figures

Figure 2.1 – Comparison of Airship with other flight platforms

Figure 2.2 - Simplified Block Diagram of Autonomous Navigation

Figure 2.3 - Simplified Block Diagram Autonomous Surveillance

Figure 4.1- PCBs that need to be built

Figure 4.2 - PIC 18F452, DIP

Figure 4.3 - CPU PCB

Figure 4.4 - GPS Receiver PCB

Figure 4.5 - Close up of 74HC08

Figure 4.6 - Motor Drive PCB and Multiple L293Ds

Figure 4.7 – MAX 232 chip

Figure 4.8 - RS 232 PCB

Figure 4.9 - Electronic Compass, CMPS03

Figure 4.10 - Placement and integration of CMPS03 on CPU Board

Figure 5.1 - Gondola, Thrust Motors and Propellers

Figure 5.2 - Geared Thrust Motors

Figure 5.3 - Servo Motor

Figure 5.4 - Rudder Force Equivalent

Figure 5.5 - New navigational bearing correction system.

Figure 5.6 - New stationary bearing correction system.

Figure 6.1 - Main Sequence of Source Code

Figure 7.1 - Mounted Wireless Camera

Figure 7.2 - Close up of Wireless Camera

Figure 8.1 – Graph of Wind Force Vs Wind Speed Sq

Figure 9.1 – Closed Loop Yaw Control

Figure 9.2 – Proportional Navigation Yaw Control

Figure 9.3 – Net Turning Moment (Stationary Control)

Figure 9.4 – Rise Time of Control System (Stationary Control)

Figure 9.5 – Proportional Thrust Control

Figure 10.1 - Off the shelf Gondola

Figure 10.2 - Modified Gondola with autonomous flight controls

Figure 11.1- Transporting the Blimp

Figure 11.2 - Blimp at NUS tennis courts

Figure 11.3 – Initial Bearing Correction

Figure 11.4 – Flying towards waypoint

Figure 11.5 – Blimp on its way to waypoint

Figure 11.6 – Blimp very close to waypoint

Figure 11.7 – Blimp hits waypoint head on

Figure 11.8 – Starting view

Figure 11.9 – Blimp still some way off

Figure 11.10 – Blimp heading closer

Figure 11.11 – Blimp very close to waypoint

Figure 11.12 – Blimp hits target

List of Tables

Table 2.1 – Comparison of Airship with other flight platforms

Table 3.1 – Parameters of GPS Modules sourced

Table 3.2 – Weighted Property Index Chart

Table 8.1 – Wind Force on Airship

Table 8.2 – Thrust Force generated by motors in the forward direction

Table 8.3 – Thrust Force generated by motors in the reverse direction

List of Symbols

$F_{T,forward}$	The thrust force generated by 1 propeller spinning in the forward direction, N
$F_{T,reverse}$	The thrust force generated by 1 propellers are spinning in the reverse direction, N
DutyCycle _{Forward}	The duty cycle output to the thrust motors when the propeller is spinning in the forward direction, %
DutyCycle _{Reverse}	The duty cycle output to the thrust motors when the propeller is spinning in the reverse direction, %
F_L	Lift Force, N
F_W	Wind Force, N
Vol	Volume, m ³
ρ	Density, mass per unit volume, kgm ⁻³
pair	Density of air at standard room temperature and pressure = 1.288 kgm ⁻³
g	Acceleration due to gravity = 9.80665ms ⁻²
C_D	Coefficient of Drag, [dimensionless]
A	Projected Surface Area, m ²
F_D	Drag Force, N
D	Diameter, m
V	Velocity, ms ⁻¹
μ	Absolute or dynamic viscosity, Nsm ⁻²
Re_c	Reynolds number

γ	Weighted Module Performance Index
β_i	Property Value
W_i	Weighting Factor
θ	Bearing

1. Introduction and Literature Review

This paper will look into the case for the development of an autonomous blimp and the actual design, fabrication, integration, testing and verification of an autonomous flight and surveillance platform.

Unmanned Aerial Vehicles (UAVs) have proofed their worth during operations in recent conflicts such as Kosovo. Being unmanned, they reduce the risk that a pilot is normally exposed to. However, autonomous unmanned UAVs are still very much in the research stage. In April 2004, Boeing concluded an autonomous surveillance on a fixed wing craft, named the “ScanEagle” (Ref. 22). This is believed to be the first autonomous launch and recovery.

The airship has a long history as a flight platform. It dates back to 1852 (Ref 12.) and was used extensively in WWI and WWII, both as a surveillance and a bomb-dropping platform (Ref. 12). However, the use of the airship suffered with the explosion of the Hindenburg in 1937. (Ref 7, 12) There has been a recent surge of interest in the use of the airship as a surveillance platform due to its cheaper cost, long operational time (Ref. 6, 14).

In the area of developing an autonomous airship, the most notable projects thus far are the AURORA (Autonomous Unmanned Remote Monitoring Robotic Airship) followed by the later LAAS-CNRS. In the AURORA project, simulation environments were created, dynamics modeled and blimp navigation strategies developed (Ref 6, 7, 9, 11).

This was followed by the LAAS-CNRS which has developed a semi-autonomous terrain mapping blimp (Ref. 10, 13). Some research has been done in cooperative search using unmanned blimps (Ref 8.).

However, the autonomous/semi-autonomous blimps developed thus far are greater than 8m in length. A blimp of such big dimensions would be limited in operational deployment in war/peace keeping operations. One of the aims of this project therefore would be to research and develop an autonomous proof of concept blimp that is significantly smaller than those developed presently.

1.1 Objectives

The primary objective of this project is to develop an autonomous, generic flight navigation and surveillance system in-house, comprising the electronic hardware, integration with actuators and developing the necessary code. Thereafter, the control system is to be fitted onto an airship and validation tests are to be done to demonstrate the viability of the system developed.

This primary objective can be broken into 3 milestones:

1. Choosing and purchasing an appropriate Global Positioning System (GPS) module, consisting of a GPS receiver and GPS antenna.
2. Performing an autonomous handheld gondola test
3. Demonstrating the autonomous navigation and surveillance capability on a suitable flight platform

1.2 Organization of Thesis

The format of the thesis can be broken down into a 14 different chapters. Chapter 1 will introduce the project and state the objectives of the project. Chapter 2 will look into the justification of using an airship by comparing against other available flight platforms for military surveillance and its mathematical modeling.

Chapter 3 will describe the choice of the GPS receiver to be used and the parameters used in its selection. Chapter 4 will look into the development of the electronic hardware necessary for electronic flight control. Chapter 5 will focus on the mechanical actuators used for the purpose of this project. Chapter 6 will describe the codes written for performing various functions and the actual source code itself. Chapter 7 will be the portion that focuses on the wireless camera system used for surveillance.

Chapter 8 will cover experiments conducted to gather wind and thrust force data and the derivation for a general equation for the maximum operating conditions of a blimp. Chapter 9 is the control portion and will illustrate the block diagram of the whole system, the derivation of a transfer function and the implementation and analysis of a proportional controller. Chapter 10 will be a description of the integration and testing of the entire autonomous flight control system. Chapter 11 will present the flight tests conducted, both indoor and outdoor. Chapter 12 will be an evaluation of the autonomous airship and will highlight characteristics of the airship. Chapter 13 will present the author's recommendation on areas of further study and development and Chapter 14 will conclude the thesis.

1.3 Acknowledgement of previous project

The author will like to acknowledge the contributions provided for by the completion of a previous project which was a study into the airship as a potential flight system for military surveillance and the development of a Remote Control (RC) blimp.

Specifically, the 2 portions that were relevant and used in this project is the mechanical support structure of the surveillance camera and the actual surveillance camera itself.

2. Choice and Analysis of Flight Platform

The flight platform chosen for this project is the blimp, which is an airship without an internal rigid structure. A vector thrust blimp was chosen as it relies solely on static lift and is able to provide a variable thrust line. An 8 foot (2.4m) long RC blimp was purchased from Canada. The main components of the blimp are:

- Gas envelope
- Gondola
- Control Hardware
- Actuators
- Tail fin stabilizers

Please refer to Appendix 2.1 for pictures of the blimp and control hardware.

2.1 Comparison against other flight platforms

The primary purpose for the autonomous airship developed in this project is for surveillance in a military context. The blimp is compared to the other 2 general categories of flight platforms available, fixed wing and rotary wing aircraft in Table 2.1 below.

Table 2.1 – Comparison of Airship with Other Flight Platforms

Parameters	Blimp	Fixed Wing	Rotary Wing
Cost	✓ Low	High	High
Power Consumption	✓ Low	High	High
Noise Signature	✓ Low	Moderate	High
Stationary Surveillance	✓ Capable	Incapable	Capable
Environmental Susceptibility	✗ High	Low	Low
Profile Size	✗ Large	Small	Moderate

Looking at the table above, we can see that some advantages of an airship as a surveillance craft are low cost, low power consumption, low noise signature and being capable of stationary surveillance. However, this must be balanced with the fact that the airship is more susceptible to environmental factors, particularly wind, and also has a large profile in comparison to the other 2 platforms.

Thus, the most appropriate setting for the use of an airship would be for the routine surveillance in a secured military area with little hostilities. As the blimp is a cheap, autonomous flight system, 1 operator can manage a number of blimps. The bird's eye view provided by the surveillance camera allows the single operator to monitor a number

of video images simultaneously. Furthermore, by being autonomous, the airship cannot be affected by frequency jamming tactics and pilot error.

2.2 Autonomous Flight Control

To achieve autonomous flight control, which also corresponds to navigating autonomously to a few waypoints in succession and conducting surveillance, a GPS module, consisting of a GPS receiver and a GPS antenna, is used as a real time position sensor, providing position data every 1 second. This position is described in terms of longitude, latitude and altitude. By comparison with the intended waypoint, the microcontroller calculates the required distance and bearing. Thereafter, the microcontroller controls the on-board actuators to face the airship in the correct bearing and to minimize the distance. Upon navigation to the waypoint, the airship will perform stationary bearing correction to bring it to face the correct survey bearing and then maintains the survey bearing for the length of the survey duration. When the airship has finished surveillance at that point, it then proceeds to the next waypoint and this continues until all waypoints have been reached, which will then mark the completion of successful flight. Figures 2.1 and 2.2 below describe the autonomous navigation and the autonomous surveillance. A more complex block diagram will be presented in Chapter 9.

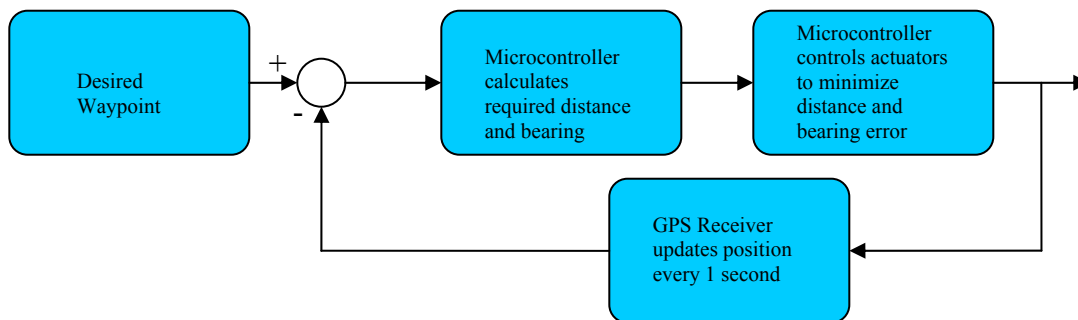


Figure 2.1- Simplified Block Diagram of Autonomous Navigation

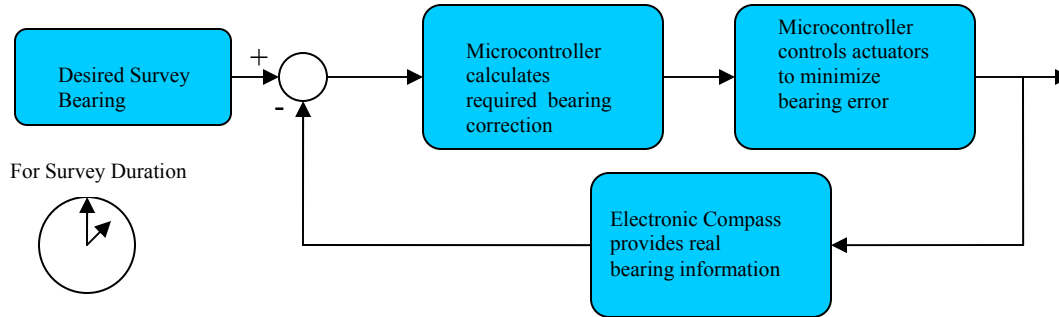


Figure 2.2 - Simplified Block Diagram Autonomous Surveillance

3. Design of GPS Navigation System

For autonomous navigation, the GPS receiver acts as the real time position sensor (Ref 1,23). The information from the GPS receiver is in the National Marine Electronics Association (NMEA) 0183 protocol, which is in the ASCII form (Ref 15). Appendix 3.1 explains the field definitions as used by the Trimble Lassen SQ, the GPS module chosen. There are a number of different formats available in the NMEA 0183, of which the GGA format, providing time, latitude, longitude and altitude is selected as it has the relevant information for autonomous navigation. See Appendix 3.2 for the GPWGA format and its fields.

3.1 Parameters of GPS Modules

As there are a number of GPS receivers in the market, the selection of the receiver was done by comparing the different systems using 6 different parameters. The 6 parameters and the rationale for their choice are as follows.

1. Weight – Because the airship can only carry a load of up to 550g, the weight becomes a critical issue. The weight of the GPS receiver and antenna is not to exceed 180g.

2. Battery Voltage – This is related to weight as the batteries form a significant percentage of the total weight. One would need more batteries for high voltage.
3. Accuracy – Accuracy is measured in CEP, the radius in which the reading obtained is 50% likely to be accurate. The higher the accuracy the better for navigation.
4. Customer support – Technical customer support is important in providing the student with needed information and help, which may lead to the development of better and more efficient solutions to problems which might be encountered along the way. Local, person to person support is preferred over overseas email support.
5. Size – Smaller components would mean more space to house other items.
6. Cost – The budgeted cost for the GPS components is \$500.

The relative importance of these 6 parameters was determined using a Relative Weighing Factor Chart (Appendix 3.3).

3.2 GPS modules sourced

After listing the 6 parameters, a total of 6 GPS modules were sourced. (See Appendix 3.4)

Their parameters are presented in the table below:

Table 3.1: Parameters of GPS Modules Sourced

GPS Module	Customer Support	Weight	Accuracy	Voltage	Size	Cost
Trimble Lassen Sq	Distributed locally by Dinkum Technologies, with support	Receiver: 5.7g Antenna: 115g	Horizontal CEP 6m Vertical CEP 11m	3.0V to 3.6V	Receiver: 26mm x 26mm x 6mm Antenna 50.5mm x42mm x13.8mm	\$102.00 for Receiver \$45 for Antenna
Motorola FS Oncore	Local Distributor. But has Minimum Order Quantity of 100.	Receiver: <10g Total: <100g	Horizontal CEP 6m	3.0V	Receiver: 14.5mmx18mmx2.75mm Antenna 38.5mm x34mm x13.2mm	Unable to Determine, But estimated to be about the same as Trimble Lassen SQ
Garmin GPS 35 TracPak	Local Distributor without technical support	110g	Horizontal CEP 15m	10V to 30V	Receiver and Antenna package: 56.4mm x 96.3mm x 26.7mm	Unable to Determine
Laipac TF30 Evaluation Kit	Overseas Distributor, with technical support via email	Unable to Determine	Horizontal CEP 25m	4.5V to 6.0V	Receiver: 30mm x 40mm x 7mm Antenna 49.3mm x49.3mm x17mm	\$321 for evaluation kit (excluding shipping)
Parvus Orbitrak 8 R	Overseas Distributor, with technical support via email	Unable to determine. Likely to be on the high side	Horizontal CEP 6m Vertical CEP 11m	5.0V	Receiver Board: 90mm x 95mm Antenna 50.5mm x42mm x13.8mm	\$556 (excluding shipping)
San Hose DGPS -220-PC	Overseas Distributor, with technical support via email	681g	DGPS. Horizontal accuracy 1 to 5m	12V to 24V	Receiver and Antenna package: Height: 82.5mm Diameter: 112mm	Unable to Determine

3.3 Analysis and Choice of GPS module

The modules chosen for comparison above are compared to one another using a Weighted Property Index Chart, presented in Table 3.2. Each of the 6 parameters were given a relative weight determined in the Relative Weighting Factor Chart drawn out in Appendix 3.3. Also, some of these parameters have a critical value that the selected GPS module must meet and this is determined in a “Go/No-Go screening”

The critical parameters which require a “Go/No-Go” screening are:

1. Weight – the combined weight of the GPS receiver and antenna must be below 180 grams.
2. Cost – the combined cost of the GPS receiver and antenna is budgeted to be below \$500.

A score between 0 and 100 is given to each of the parameters, which when multiplied with the Relative Weight of the parameter and summed will give the Performance Index:

$$\gamma = \sum \beta_i W_i$$

A score of “50” is given to parameters which have been labeled “Unable to Determine”

A “S” is given for modules which have satisfactorily passed the critical parameters and a “US” is given for those which fail in that parameter. Modules must pass all critical parameters. Appendix 3.5 shows the comparison of the various GPS modules using “A Go/No Go & Weighted Property Index” Chart.

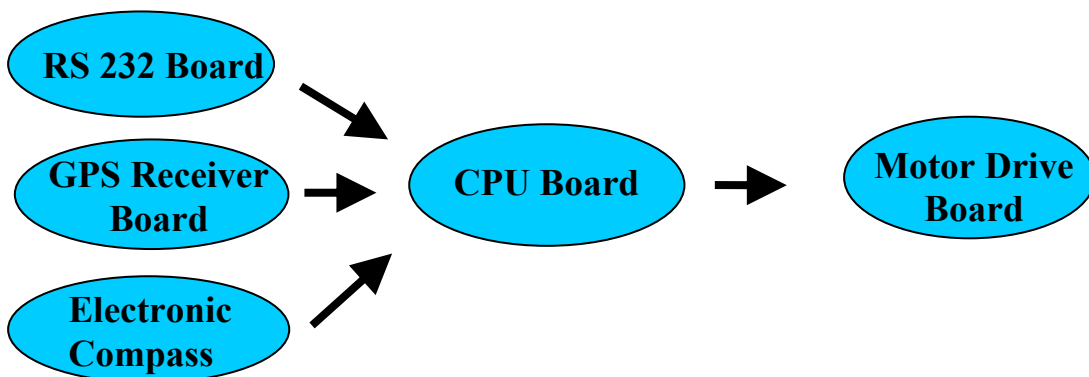
The GPS module comprising a Trimble Lassen SQ GPS Receiver and a Shielded Magnetic Mount Antenna, has the highest Module Performance Index of 96 out of a possible 100, and is selected. A technical drawing of the Lassen SQ is attached as

Appendix 3.6. Also, a technical drawing of the Magnetic Mount Antenna is attached as Appendix 3.7.

4. Design and Fabrication of Electronic Hardware

A broad description of the function that the electronics hardware together with the source code is to achieve is to be able to read desired positions (called waypoints and specified in terms of latitude, longitude and altitude). It then compares the desired waypoint with the current position sensed by the GPS receiver and it is then to compute the required distance and bearing. This is very similar to the concept of polar coordinates. North has a bearing of being 0° and South 180° . The current bearing is sensed using an electronic compass. Following which the electronics must then output the correct controls to drive the various motors to minimize the errors in distance and bearing, so that the airship will be propelled towards the waypoint. To implement the above functions, the various boards have been built and integrated as shown in the figure below.

Figure 4.1- PCBs that need to be built



These boards were built after breadboarding. The design of the 4 Printed Circuit Boards (PCBs) were done using Protel Design System. The design was then sent to the PCB Fabrication Lab in NUS to be produced. The various components of the PCBs were then soldered on.

4.1 Microcontroller Board

The Central Processing Unit (CPU) board is at the center of the entire electronics, receiving position and bearing information, computing required distance and bearing and controlling the motors appropriately.

The PIC microcontroller was chosen to implement this CPU function. It is readily available, cheap, easy to use and is also used widely in the NUS EE department. 3 different variations were tried: the Basic Stamp 2sx, the PIC 16F877 and the PIC 18F452. Because of the limitations in Random Access Memory (RAM) of the previous 2 microcontrollers, which is needed to hold the variables declared in the source code such as waypoints, the PIC 18F452 was chosen (See Figure 4.2). It has 1536 bytes of RAM which allows the user to declare up to a maximum of 50 different waypoints. It is also cheap, at \$15 from Farnell-Newark and comes in Dual In-line Package (DIP) which allows for easy development by use of a breadboard.

After breadboarding, a Printed Circuit Board (PCB) was designed and built around the microcontroller. The functions provided are: a programming input port, a regulated voltage, input/output connections, a mechanical power switch, and 4 signal Light

Emitting Diodes (LEDs). The Protel Design of the CPU board is attached as Appendix 4.1. Also, Appendix 4.2 explains the various components in the CPU PCB.



Figure 4.2 - PIC 18F452, DIP



Figure 4.3 - CPU PCB

4.2 GPS Receiver Board

The GPS receiver board was built to interface the Trimble Lassen SQ GPS receiver with the microcontroller. Figure 4.4 is a photo of the GPS receiver PCB. This is to establish 2-way communication, for the microcontroller to read the NMEA 0183 GGA output from the GPS receiver and for the microcontroller to be able to be used to program the GPS receiver. A disparity exists between the high state voltage of the GPS receiver (3V) and what the microcontroller recognizes as high (CMOS technology, >3.7V). See Appendix 4.3 for a table that explains the logic formats. A 74HC08 chip was used to drive the high state of the GPS receiver to 5V for

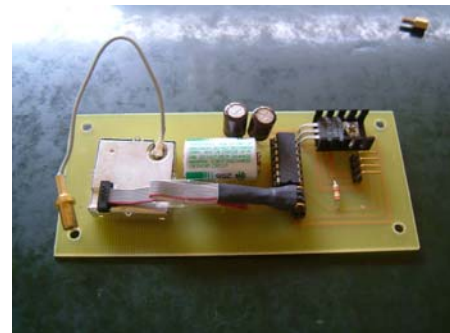


Figure 4.4 - GPS Receiver PCB

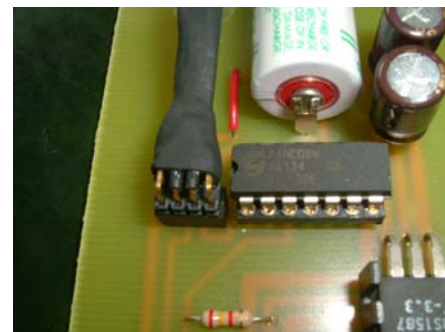


Figure 4.5 - Close up of 74HC08

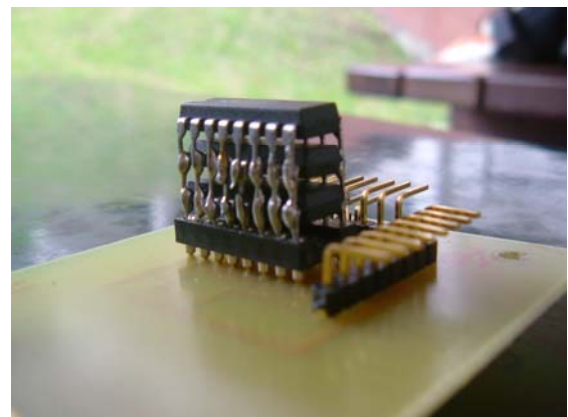
correct communication. Figure 4.5 is a close up shot. There is also a 3V voltage regulator, LMS 1587-3.3ct which is used to correct 5V input to the 3.3V power needed by the GPS Receiver. Also, there is a standby Li-Ion battery, which is sufficient to last for 2 years, and it serves the purpose of reducing the warm up time needed by the Lassen SQ from 2 minutes to 20 seconds.

As stated in the beginning of the chapter, the design of the GPS Receiver PCB was done in Protel and is attached as Appendix 4.4. Also, Appendix 4.5 explains the various components used in the GPS receiver board.

4.3 Motor Drive Board

The microcontroller is the chip that outputs the voltages to control the motors appropriately for autonomous navigation. However, the maximum current output of the Input/Output pins of the PIC 18F452 is 25mA. This is insufficient to drive motors, which often required currents in excess of 1A. Therefore, a channel driver was needed to increase the current available to the motors, with the signals from the microcontrollers serving as the switching signals. The L293D, which is a 4 channel driver with diodes, was chosen. Each chip has 600mA output current capability per channel, with a peak output of 1.2A current (non-repetitive).

Testing the current draw of the thrust motors used in the airship determined that each motor requires a current of 2.2A at maximum duty



cycle. Therefore, a quick and effective way was used to accommodate provide this current level. 3 L293D chips were soldered one on another, enabling them to act as parallel current sources so that the individual chips do not overheat, as seen in Figure 4.6. The design of the Motor Drive PCB is attached as Appendix 4.6 and the components of the Motor Drive PCB are explained in Appendix 4.7

4.4 RS-232 Interface Board

The microcontroller needs to be able to communicate with the laptop for the purpose of inputting the desired waypoints and authentication. Input and outputs to and from a laptop are often by a RS 232 cable. The specifications of the RS 232 format is that -5V to -12V is recognized as a high “1” while + 5V to + 12V is taken as a low “0”, which can be seen in Appendix 4.8. Compared to the CMOS format used by the microcontroller, where 3.7V to 5V is taken as a high and 0V to 1.3V is taken as a low (See Appendix 4.3), there is a difference. Therefore, a MAX 232 chip was used as a RS 232 driver, effectively allowing the laptop to communicate with the microcontroller.

The other component on the RS-232 board is a single pole, double throw mechanical switch. This is used as there is a need to change between the microcontroller serial receive pin (Rx) being connected to the MAX 232 chip, during authentication and waypoint input, to being connected to the GPS Receiver output pin for autonomous navigation. Figure 4.8 is a photo of the RS 232 PCB. The Protel design of the RS-232 PCB is attached as Appendix 4.9. Appendix 4.10 shows the various components of the RS-232 PCB.

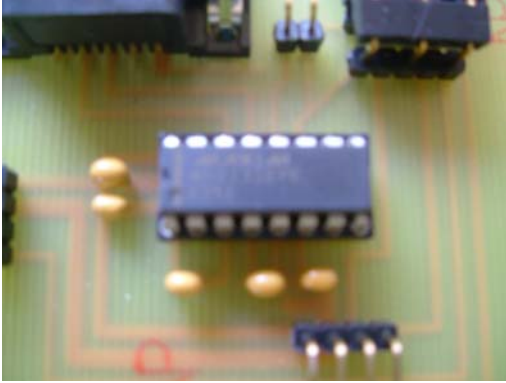


Figure 4.7 – MAX 232 chip

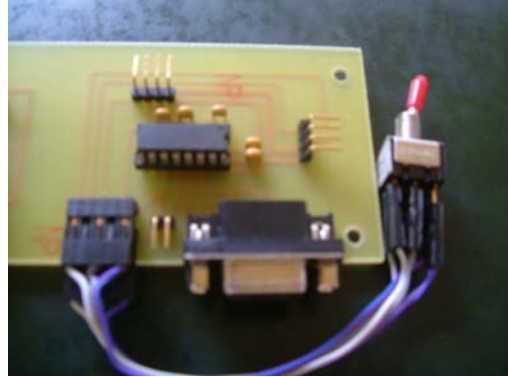


Figure 4.8 - RS 232 PCB

4.5 Electronic Compass

As described in the beginning of this chapter, the airship navigates by minimizing the error between the desired and actual position and bearing. While the GPS module provides real time position updates, the current bearing is provided by an electronic compass.

The CMPS03 (Figure 4.9) was chosen as the electronic compass to be used as it provides bearing outputs to a precision of 0.1° and is easy to integrate with the PIC 18F452 via the I²C protocol. However, it is sensitive to the EM field generated by the PCB boards and care was taken in its placement to minimize any unwanted effects on reading. Figure 4.10 shows the placement and integration of the CMPS03 with the CPU PCB.



Figure 4.9 - Electronic Compass, CMPS03

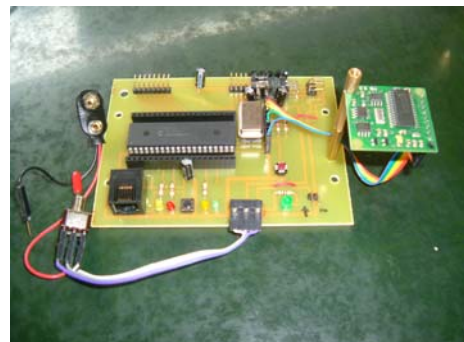


Figure 4.10 - Placement and integration of CMPS03 on CPU Board

5. Modification of Mechanical Actuation

The off the shelf RC blimp has 3 DC motors and 1 servo motor. There are 2 smaller DC motors which serve as thrust motors, enabling forward motion control. Figure 5.1 shows the gondola and the thrust motors. They are controlled by the same signal from the remote controller and have either an “on” state or an “off” state. On its own, each small DC motor draws 2.1A at 7.2V. They are also geared to the propellers at a ratio of 42:10 which provide the thrust force.



Figure 5.1 - Gondola, Thrust Motors and Propellers



Figure 5.2 - Geared Thrust Motors

The line of thrust of the thrust motors is determined by the position of the servo motor, seen in Figure 5.3. The position of the servo motor in the off-the-shelf system was controlled by the remote controller. There is a gear ratio of 10:20, allowing for deflections of -90° to $+90^\circ$. Control of this servo motor is now modified to be by the microcontroller

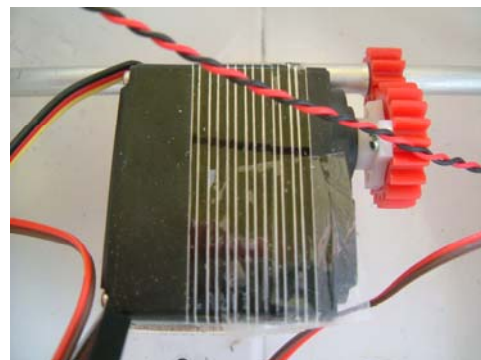


Figure 5.3 - Servo Motor

and is enabled by a software-enabled Pulse Width Modulation (PWM) signal. The code has been written as part of this project in C language. This will be discussed in deeper detail in Chapter 6.2.3. A carbon fiber rod on bearings reduces friction during the changing pitch angle of the thrust force.

Yaw control in the RC blimp system, which is the horizontal direction the blimp is facing, is enabled by a larger DC motor with a 6-9 propeller acting as the rudder. This DC motor draws 4.5A at 7.2V.

5.1 Rudder Motor Approach

As described above, the yaw control is achieved by the larger DC motor. This can be represented diagrammatically as shown in figure 5.4. As can be seen from the figure, when the rudder motor exerts a force to turn the blimp, this is equivalent to both a turning moment and a sideways force acting at the center of gravity of the blimp. Thus the blimp not only turns, it also moves sideways when doing bearing correct. Also, this means that with this system of having a single rudder motor, the blimp is incapable of doing stationary bearing correction. This observation has been observed during the flight tests conducted.

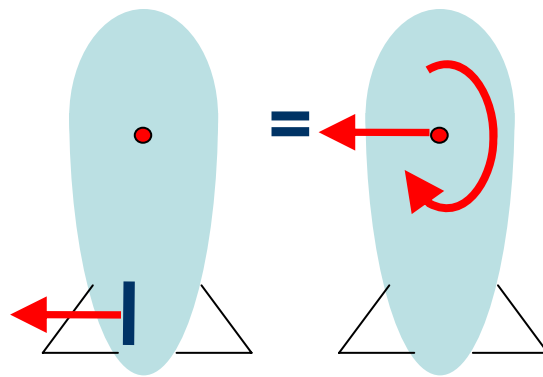


Figure 5.4 - Rudder Force Equivalent

5.2 A Better System -Bi-directional Thrust Motors

Thus a new system for bearing correction had to be designed and implemented. The issue of bearing correction could be divided into 2 main portions: bearing correction during navigating and bearing correction during on-the-spot surveillance. What is practical during navigational bearing correction is that the airship should still have a forward thrust force component while having a turning moment, which draws similarities to one making a slight direction change when driving a car. However, in the case of stationary surveillance at designated waypoints, the system should only provide a turning moment and no resultant forces at the Center of Gravity (CG).

It would take much effort to design and integrate an entirely new system. Thus, it was more practical to design a method and implement it using the current system. The 2 geared DC thrust motors-propellers setup were modified to achieve the aims above.

Firstly, their connections have been separated such that they now function independently.

Furthermore, the code for a PWM signal by the microcontroller to provide a variable voltage to the thrust motors via the concept of the duty cycle was written (See Appendix 5.1 & Ref 5))

They are also now able to generate a backward thrust force. Essentially, this means that the thrust motors are now independent, bi-directional and have variable speed control.

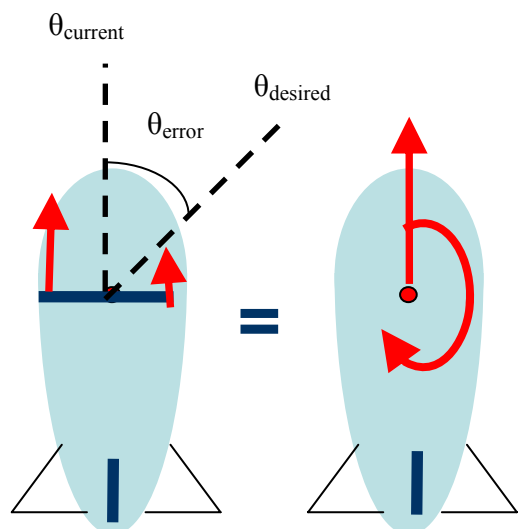


Figure 5.5 - New navigational bearing correction system.

For bearing correction during navigation, both motors turn to generate a forward thrust force. However, one of them turns at a slower rate such that there is a net moment generated, turning the airship. Figure 5.5 shows the system generating a forward force and a moment that turns the airship clockwise. The left hand motor is at the maximum of 100% duty cycle. The voltage to the right thrust motor is variable, allowing the microcontroller to control the thrust force generated by the right motor. A proportional controller was implemented to maximize the turning moment when θ_{error} is big and decreases the moment proportionally as θ_{error} decreases. For clockwise turning, left hand motor is at the maximum of 100% duty cycle. The duty cycle to the right hand motor is given by the equation:

$$Duty\ Cycle = 100 - 100 * \theta_{error} / \theta_{bearing_upper_limit}$$

For stationary bearing correction for on-the-spot surveillance, the microcontroller turns both motors in opposite directions, generating an equal thrust force. This gives rise to a turning moment without any resultant force acting on the airship. This concept can be demonstrated in Figure 5.6.

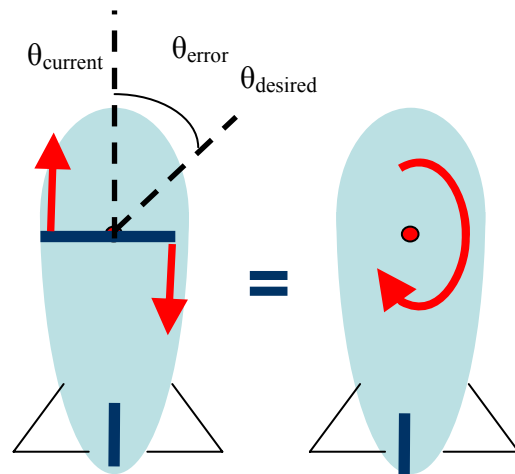


Figure 5.6 - New stationary bearing correction system.

5.3 Analysis and Choice of approach

Therefore, because of the reasons presented in Chapter 5.1 and 5.2, the new system of modifying and using 2 independent, bi-directional and variable speed thrust motors allows both turning without drift and stationary turning. Therefore, it is favored over the system that was bought off-the-shelf.

Furthermore, as the rudder motor is now not being used, the payload gained by removing it can be used to install stronger thrust motors. Also, the rudder motor now no longer draws 4.5A at 7.2V, equating to a longer operational flight time as the current draw on the Li-Ion battery is reduced. The line of thrust of the 2 thrust motors is determined by the servo motor, which is now controlled by the microcontroller.

6. Development of Source Code

Programming of the microcontroller, the PIC 18F452, is essential for the flight system to be able to operate autonomously, independent of human control (Ref 4.). It specifies what inputs the system are to take in, at what intervals, what the information that comes in relate to, how they are compared, what control actions are needed, and then outputting the required actions so as to achieve the desired operation.

The operation required of the flight system in this project, in collaboration with HQ SCE, is for the user to be able to input a number of waypoints, and the flight system is then to fly to these waypoints sequentially and conduct stationary surveillance in a specified

bearing for a specified time at designated waypoints. The source code written, together with the hardware and actuators, is able to perform the required operation.

Programming of the microchip is done using a MPLAB ICD2 programmer and debugger, which was bought at Farnell-Newark.

6.1 Choice of programming language

C language was chosen as the programming language. The reasons that led to this choice are:

- C language has a mathematics library which allows for the easy usage of mathematical functions required for autonomous navigation such as arctan, sin and cos.
- C language is considered the high language (ease of human usage) among the low level languages (more efficient code). This allowed me to write code easily and at the same time, have enough low level control on the code.
- C language is widely used and there are a number of user forums on code written in C language.

Thus, a “C language” software was bought for use in the MPLAB environment. It is CCS C compiler, works for all PIC microcontrollers and cost \$1,200.

6.2 Function Development

As the source code required a number of different functions, these functions were built independently initially and tested to ensure that they were working well together with the hardware.

6.2.1 Lighting LEDs with timing control

A code was written to verify the microcontroller could be program as well as implement the basic functions required, digital input-output as well as timing control. The code is attached as Appendix 6.1

6.2.2 Serial Transmit and Receive

As there is a need to transmit and receive information over the serial interface, we must initialize the system appropriately. The code attached in Appendix 6.2 is to be used together with the RS-232 PCB described in Chapter 4.4.

6.2.3 Servo and DC Motor Control

In the off-the-shelf system, the servo motor in the airship was controlled by a human using a remote controller. With the removal of the human and remote control element, a code is written to allow the microcontroller to control the position of the servo motor.

Essentially, the position of the servo motor is controlled by the length of the high period of the pulse wave. Also, the servo motor needs a PWM that has a frequency of at least 50Hz. The PIC 18F452 only 2 PWM pins which are being used for the control of the 2

thrust motors, therefore a software PWM, allowing the generation of a PWM signal over a normal digital I/O pin.

Originally, all three of DC motors were controlled by an “on” or “off” signal sent by the remote controller. This function is replaced by microcontroller, outputting the on-off signals via I/O pins. The code for the control of servo motor and on-off control of DC motors is attached as Appendix 6.3

6.2.4 Variable DC Motor Speed and Direction Control

The on-off DC motor control action is for the old system of actuation as described in Chapter 5.1. However, because of the adoption of the design explained in Chapter 5.2, a new code needs to be written to allow the microcontroller to control the DC thrust motors independently, in both directions of rotation and at varying speed. The code written for this purpose is attached as Appendix 6.4

6.2.5 Bearing reading from electronic compass

The electronic compass, CMPS03, outputs the bearing of the airship to be read by the microcontroller for control action. The bearing can be read in 2 forms, a PWM and an I²C output. The I²C output is chosen as this is more precise and generates less overhead for the microcontroller. There are 2 choices in the I²C output form, data in the form of a byte which gives an accuracy up to the nearest 1.40625°, and a long integer which gives accuracy up to 0.1°. The code for reading the current bearing provided by the CMPS03 is attached as Appendix 6.5

6.2.6 Reading GPS coordinate outputs

Since the current position of the airship is vital to autonomous navigation, the microcontroller needs to be able to read in the position data from the GPS receiver, which has been integrated into the GPS receiver board as mentioned in Chapter 4.2. They communicate via the serial data receive and transmit system and the code is attached as Appendix 6.6.

6.3 Overview of Source Code

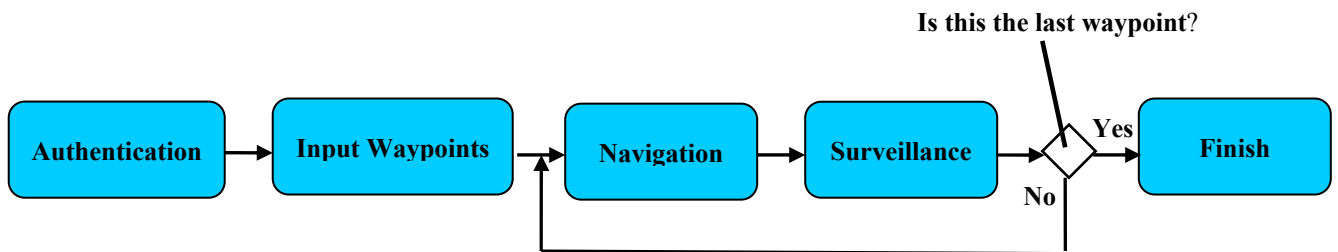


Figure 6.1 - Main Sequence of Source Code

The main sequence of the main source code can be described with the use of Figure 6.1. The code starts off by authenticating the user with a 4 digit password. If the user enters the correct password, the user can then enter up to 50 waypoints, specifying their latitude, longitude, altitude, whether it is to be a designated survey point, and if it is, the survey bearing direction and the duration of survey. Once the user has finished entering all the desired waypoints, the blimp will commence flight navigation when it is able to receive GPS signals. It then flies autonomously to the current waypoint and surveys there for the required duration. This cycle continues until the airship has successfully navigated to all

the waypoints, at which point the code will end, signifying the end of the flight operation. The entire source code was developed for this project and is attached as Appendix 6.7.

6.4.1 Authentication

The authentication function is where the system authenticates the user, in the event that the airship falls into unauthorized or enemy hands. The password chosen is a 4 digit password.

6.4.2 Waypoint Input

The waypoint input function is where the user inputs all the required details of the various waypoints he wishes the airship to navigate to and survey. Each waypoint has been designed as a Structure called “point” in C programming and the fields in each waypoint are latitude, longitude, altitude, to_survey, survey duration and survey bearing. The commands also give specific formats for entering these details. At the end of entering a waypoint’s details, the user is given the opportunity to check through them, and edit them if they are not correct. The code is also designed to retain the number of waypoints the user has entered for flight navigation purposes, which means the user need not spell out how many waypoints he wishes the system to fly to.

6.4.3 Navigation

The navigation algorithm is a closed loop control which minimizes the distance error between the current position and the desired position to within a tolerance level specified in the code. The current position is received from the GPS receiver and the GPGGA

format is used. From this length of characters, the current latitude, longitude and altitude are derived and used for comparison. Initially, the code is written such that the airship performs a stationary bearing correction, explained in Chapter 5.2 to within a initial bearing tolerance, which has been specified to be 30° . When this is done, the airship commences flight towards the waypoint. Each loop of checking its current position is every 1 second due to the specifications of the Trimble Lassen SQ. During each loop, the airship calculates its distance to the waypoint and its desired bearing. It flies towards the waypoint and does in-flight bearing correction as explained in Chapter 5.2. This looping process continues until the airship senses that it is within a specified tolerance distance of the waypoint, at which point it is deemed to have reached the waypoint. Following this, it commences on the spot surveillance if it is a designated surveillance point or if not, it navigates to the next waypoint.

6.4.4 Stationary Surveillance

.If the waypoint has been designated as a surveillance waypoint, the code is written such that the airship performs a stationary bearing correction to reach the survey bearing, within a specified survey tolerance. Once it reaches within this tolerance, the code starts timing until the survey duration is completed. At the same time during the running of the internal clock, the airship constantly checks its current bearing and ensures that it is within tolerance of its survey bearing. At the end of this survey duration, the airship then navigates to the next waypoint.

7. Surveillance System

The surveillance system comprises of a wireless video camera, the transmission receiver and the hardware and software to display the image onto the screen of a laptop.

7.1 Wireless Camera and Receiver

The wireless camera and transmission receiver were chosen as part of the previous thesis. Its resolution capability was also determined in the previous project and is attached as Appendix 7.1. For the purpose of this project, the power source chosen was its own 9V battery as it was found that the transmission had a lot of interference when using power tapped from the CPU board. A single pole, double throw mechanical switch was also used so that the user powers both the CPU board and the wireless camera at the same time. Modification of the power supply of the transmission receiver was also done so that it could now be used out in the field and is not confined to a power point as it had been previously. The wireless camera was also mounted at the bottom of the gondola, as can be seen in Figure 7.1. Figure 7.2 shows a close up photo of the wireless camera.



Figure 7.1 - Mounted Wireless Camera



Figure 7.2 - Close up of Wireless Camera

7.2 Receiver Hardware and Software

As the user needs a laptop to program the waypoints into the airship in the field during surveillance operations, it was decided that it was practical to have the transmitted images displayed on the laptop screen. For this, a Video On Line hardware and software system was loaned and found to be very useful. The videos from the video camera recorded on the laptop demonstrating the effectiveness of the flight system for surveillance were done using this hardware and software.

8. Scaling up of System for Operational Deployment

As this project was sponsored by HQ SCE for the purpose of evaluating the airship as a possible platform for operational deployment, it is necessary to establish a guideline on the maximum operating conditions for an airship of a given size. While an in-depth research in this area is beyond the scope of this thesis, nonetheless, some quantification is provided.

8.1 Wind Force Determination

The main environmental factor that determines the operational capability of the airship is the speed of the wind. It is necessary to quantify the maximum wind speed that an airship can operate under. Readings of the wind force were taken to establish this relationship.

Table 8.1 shows the force exerted on the blimp by head winds of various speeds.

Table 8.1 Wind Force on Airship

Force/g	Force/N	Wind speed/ms ⁻¹	Wind Speed sq/m ² s ⁻²
20	0.1962	1.2	1.44
25	0.24525	1.5	2.25
35	0.34335	1.2	1.44
45	0.44145	1.8	3.24
50	0.4905	1.6	2.56
60	0.5886	2.1	4.41
70	0.6867	2.2	4.84
80	0.7848	2	4
90	0.8829	2.4	5.76
120	1.1772	3	9
150	1.4715	2.9	8.41
150	1.4715	2.5	6.25
160	1.5696	2.8	7.84
220	2.1582	3.5	12.25
250	2.4525	3.6	12.96
250	2.4525	3.1	9.61
280	2.7468	3.6	12.96
300	2.943	4.1	16.81
420	4.1202	4.1	16.81

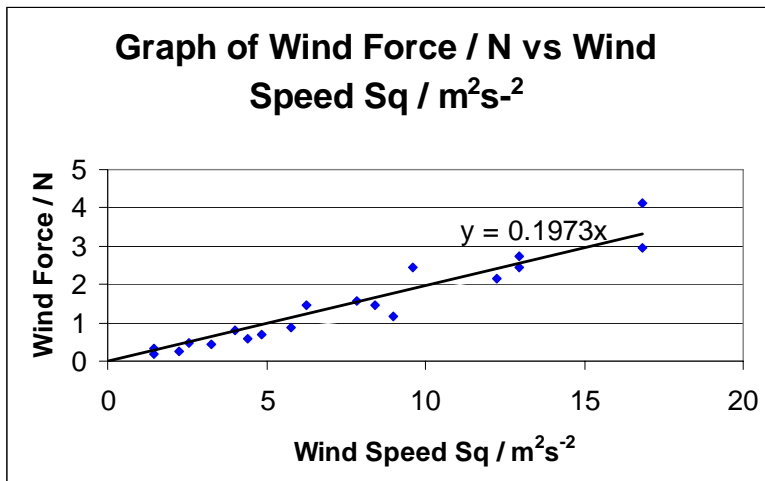


Figure 8.1 shows the graph plotted from the data obtained experimentally in Table 8.1. This graph is also attached as Appendix 8.1.

Figure 8.1: Graph of Wind Force vs Wind Speed Sq

As can be seen from the graph in Figure 8.1, the equation relating wind force to wind speed is given by:

$$F_w = 0.1973V^2$$

We also have the equation for drag force for a body in air:

$$F_D = \frac{1}{2} C_D \rho_{air} A V^2$$

Using these 2 equations, we obtained a value for $C_D = 0.26$.

Appendix 8.2 shows the derivation of this relationship which can be used for estimating the wind force on a dynamically similar airship (Ref 2). The wind force acting on a blimp which is dynamically similar to the 8 foot model used, under different wind velocities is given by the equation:

$$F_w = \frac{1}{2} C_D \rho_{air} A V^2 = 0.166 A V^2$$

8.2 Thrust Force Measurement

If thrust force provided by the propellers is greater than the headwind force acting on the airship, then the airship can navigate to the desired waypoints. Thus the thrust force generated by the propellers was quantified. Table 8.2 presents the force generated when the propellers are spinning in the forward direction, while Table 8.3 shows the force generated when the propellers spin in the reverse direction. Appendix 8.3 and 8.4 show the graphs of the Thrust Force by 1 Motor Vs Duty Cycle.

Table 8.2 Thrust Force generated by motors in the forward direction

Duty Cycle	Force/N (by 2 motors)	Force/N (by 1 motor)
100%	0.44145	0.220725
90%	0.36297	0.181485
80%	0.32373	0.161865
70%	0.26487	0.132435
60%	0.21582	0.10791
50%	0.15696	0.07848
40%	0.08829	0.44145
30%	0.03924	0.01962
20%	0	0
10%	0	0
0%	0	0

Table 8.3 Thrust Force generated by motors in the reverse direction

Duty Cycle	Force/N (by 2 motors)	Force/N (by 1 motor)
100%	0.23871	0.119355
90%	0.20928	0.10464
80%	0.18639	0.093195
70%	0.1635	0.08175
60%	0.12753	0.063765
50%	0.09483	0.047415
40%	0.06213	0.031065
30%	0.0327	0.01635
20%	0.01308	0.00654
10%	0	0
0%	0	0

From Appendix 8.3 and 8.4, the thrust force in the forward and reverse directions can be described as:

$$F_{T,forward} = 0.0028 \times DutyCycle - 0.065 \quad , \text{Duty Cycle} > 23.2\%$$

$$, 0\% < \text{Duty Cycle} < 23.2\%$$

$$F_{T,reverse} = 0.0015 \times DutyCycle - 0.0248 \quad , \text{Duty Cycle} > 16.5\%$$

$$, 0\% < \text{Duty Cycle} < 16.5\%$$

Therefore the maximum operating conditions for the current flight platform is calculated to be:

$$V_{W,\max} = 1.5ms^{-1}$$

The relevant working is provided in Appendix 8.5.

The general equation for calculating the maximum operating conditions for a dynamically similar platform is

$$V_{\max} = \sqrt{12.05 \times \frac{F_{T,\max}}{A}}$$

The relevant workings are attached as Appendix 8.6

This information is also used in implementing a proportional controller for stationary bearing correction. See Chapter 9.3.

8.3 Weight considerations

While it is desirable to have big motors and strong propellers to generate a large force to counter wind effects, in reality this is limited by the payload that a blimp of a given size can carry. Thus, a study into the payload considerations was carried out and the weights of the various components have been tabulated. Appendix 8.7 shows the weights of components which are necessary to autonomous flight navigation and surveillance and remain the same regardless of the size of the airship used, while Appendix 8.8 shows the weights of the components which will change with the size of the platform used, as well as components which are optional.

The payload of airships of various sizes is the limiting factor and quantification is provided for airships of length between 8 feet, which is the current system, and 13 feet, which is the maximum size allowed as defined by the project sponsor as being tactically deployable.

The payload information is gathered from Mobile Airships Inc, a Canadian-based company who is the supplier of the current blimp. This information has been analyzed together with the weights of the various components shown in Appendix 8.7 and Appendix 8.8 and is presented in Appendix 8.9.

The available payload for airships of different sizes, shown in Appendix 8.9, can be used for carrying thrust motors, motor holders, propellers and batteries. This can be used to increase the airship' maximum operating conditions. Also, the capacity of the batteries carried will determine the operation flight time. The cost for the airship gas bags has also been quoted by Mobile Airships Inc.

9. Design and Verification of Control System

The autonomous flight navigation and surveillance is essentially a closed loop control process in which flight platforms compares its desired waypoint with its current waypoint, and acts to minimize this error. A block diagram for the GPS Navigational Control Loop has been drawn and is attached as Appendix 9.1

9.1 Obtaining Transfer function

As can be seen from Appendix 9.1, there is a need to design and implement a closed loop yaw control. A proportional closed loop yaw control as shown in Figure 9.1 was implemented. The transfer function of the plant was first established experimentally. Appendix 9.2 shows the output response of the Plant to a step input. Complex RF, an optimization method was used to model the curve. The equation of the model curve is:

$$\theta(t) = 0.9283e^{0.4341t} + 7.4780e^{-0.1389t} + 18.1052e^{-0.8570t} + 4.8535e^{-0.5598t} + 12.6823t - 31.4568$$

The actual curve and the modeled curve plot is attached as Appendix 9.3. The transfer function of the Plant was derived and the relevant workings are shown in Appendix 9.3.

The transfer function is

$$T(s) = \frac{\theta(s)}{V(s)} = \frac{100 \times (12.6823s + 45.68127s^2 + 66.66233s^3 + 13.46875s^4 - 13.4969s^5 - 3.26738s^6)}{s^4 + 1.1216s^5 + 0.001213s^6 - 0.22705s^7 - 0.02893s^8}$$

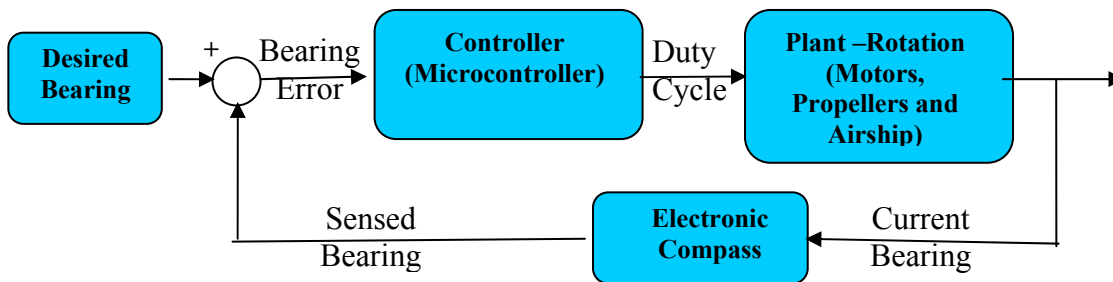


Figure 9.1 Closed Loop Yaw Control

9.2 Implementation of proportional yaw control (during navigation)

A proportional yaw control during navigation is implemented using the microcontroller. Since there are 2 motors, the microcontroller outputs a different duty to each motor, based on proportional control with saturation. The duty cycles to each motor is attached as Appendix 9.5. Figure 9.2 shows the difference in the duty cycles between the left and right motors, which is also proportional to the net turning moment of the airship.

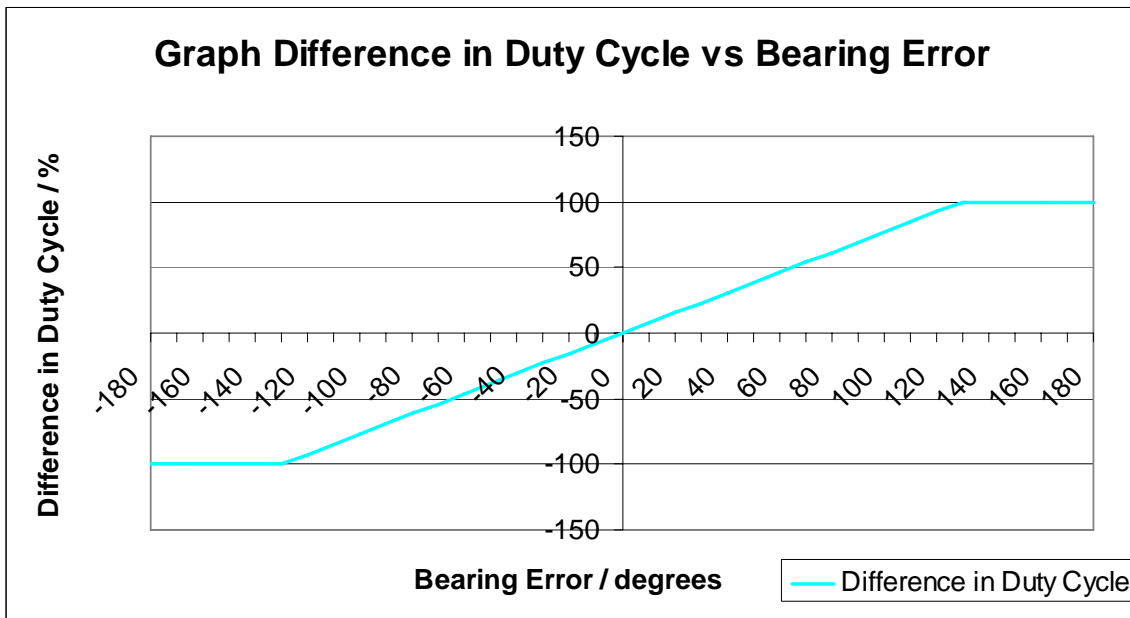


Figure 9.2: Proportional Navigational Yaw Control

The gain of the system is set at $0.741\% / ^\circ$. It has been coded such that this gain can be easily adjusted with the use of a “#define BEARING_UPPER_TOL 130.0”

9.3 Implementation of Proportional Yaw control (Stationary Surveillance)

From Chapter 8.2, we obtained the formula relating the forward thrust force and the reverse thrust force. Thus, for stationary bearing correction:

$$F_{T,forward} = F_{T,reverse}$$

$$0.0028 \times DutyCycle_{Forward} - 0.065 = 0.0015 \times DutyCycle_{Reverse} - 0.0248$$

$$DutyCycle_{Forward} = 0.5357 \times DutyCycle_{Reverse} + 0.069$$

$$F_{T,forward} = K \frac{bearingdiff}{BEARING_UPPER_TOL_STA} \Rightarrow K = F_{T,forward,max} = 0.1252$$

$$\Rightarrow DutyCycle_{forward} = 44.7 \times \frac{bearingdiff}{BEARING_UPPER_TOL_STA} + 23.2$$

$$\Rightarrow DutyCycle_{reverse} = 83.5 \times \frac{bearingdiff}{BEARING_UPPER_TOL_STA} + 16$$

As before, we want the airship to turn at a maximum rate till it reaches a bearing error θ , at which point it will execute proportional yaw control. Currently this θ is set at 30° and is easily adjustable with the line `#define BEARING_UPPER_TOL_STA 30.0`

The gain currently set is $Gain = 0.001461 Nm^{-1}/^\circ$. Appendix 9.6 shows the duty cycle to each motor to achieve proportional control with this Gain setting. Figure 9.3 shows the net turning moment being a proportional function of the bearing error, up to a maximum and minimum at which it saturates.

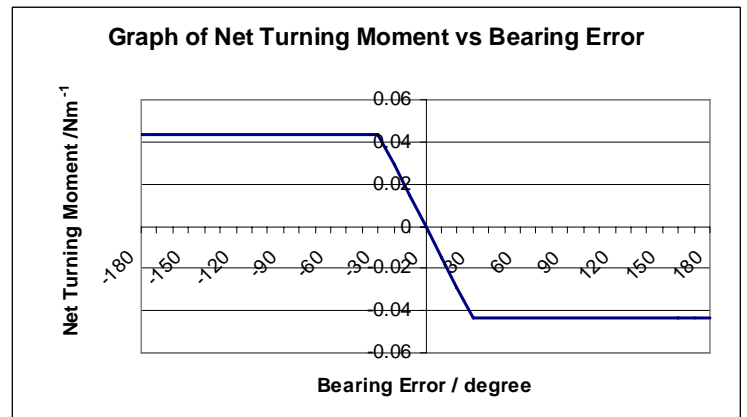


Figure 9.3: Net Turning Moment (Stationary Control)

The rise time of the control system was also determined. Looking at Figure 9.4, the system reaches 10% of its final value at $t=3s$ and 90% of its final value at $t = 18.5$ seconds.

$$\therefore RiseTime = 18.5 - 3 = 15.5seconds$$

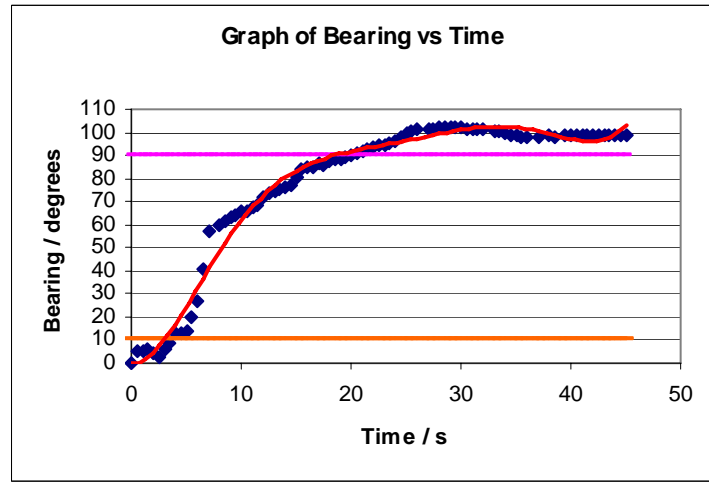


Figure 9.4: Rise Time of Control System (Stationary Control)

A bigger picture of the graph is shown in Appendix 9.7.

9.4 Implementation of Proportional Thrust Control

The thrust is also controlled using a proportional controller. As it gets closer to the waypoint, beyond a certain defined point, the thrust motors slow down proportionally. As can be seen from Figure 9.5, the gain is set to 5.

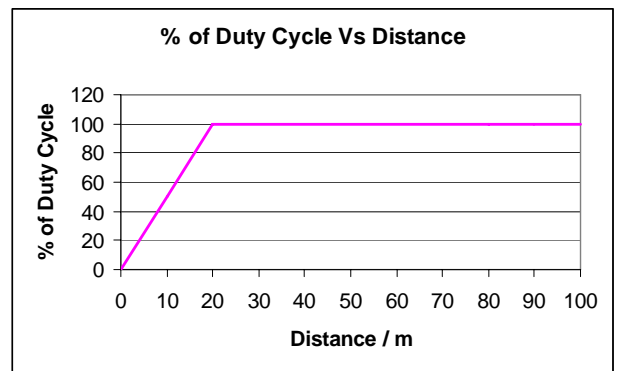


Figure 9.5: Thrust Proportional Control

10. System Development and Integration

The entire flight navigation and surveillance system was designed and developed as part of this project, comprising of electronic hardware, mechanical actuators and code as explained in Chapters 4, 5 and 6. The building of the entire system was done in stages, progressing from breadboard development, temporary gondola testing and verification to the purchase and fitting into the actual gondola to be used.

10.1 Breadboard Development

Breadboard development was the first stage in the entire process. Its purpose was to choose the correct components of the electronic hardware and connect them appropriately. The components connected to the breadboard were the PIC18F452, an oscillator, voltage regulator, and LEDs, the MAX232 and its associated RS 232 interface port, the L293D and its connections for driving motors, the electronic compass and lastly the GPS receiver and antenna. It was also during this period that the various functions listed in Chapter 6.2 were programmed into the microchip and the responses checked to ensure that the hardware and software were meeting expectations.

10.2 Temporary Gondola Verification

With the knowledge that the individual components of the entire circuit setup were properly connected, the next objective was to start building the source code for autonomous flight and surveillance function by function and verify it in a practical setting. The authentication function and authentication were developed and verified indoors. After that, the navigational and surveillance functions were developed, and this had to be verified and debugged outdoors as GPS coordinates were required. Also, the source code in these portions was coded such that important information were regularly printed to the laptop, providing a clue on whether the code was working well and which parts needed to be changed. When the various functions were properly coded, a temporary gondola was made and it housed the breadboard developed in Chapter 10.1, the GPS antenna and the various motors (at this point the thrust motors and rudder concept explained in Chapter 5.2 was being used). This temporary housing allowed for

easy hand held tests to be conducted outdoors. When possible, the temporary housing and a laptop were placed on a trolley that allowed for easy movement and easy debugging. The trolley was used as a simulated flight platform. At the end of this phase, the electronic components which needed to be used were certain and design of the actual PCBs in Protel could be done.

10.3 Integrating into Actual Gondola

The PCB boards to be designed were developed as separate boards, to allow easy modification and debugging in the future. Therefore, it was decided that 4 circuit boards were to be designed and built, each one having a specific role. Thus the CPU board, the RS-232 board, the Motor Drive Board and the GPS receiver board explained in Chapter 4.1 to Chapter 4.4 were designed in Protel. Their designs are attached as Appendices 4.1, 4.4, 4.6 and 4.9. The designs was done such that the PCBs could be stacked one on another to give the entire electronic hardware a cuboid shape that was to fit in the actual gondola. The PCBs were also designed such that the connections between the various boards were designed such that it would be practical and easy to connect. Also, the supplier of the airship, who was based in Canada, was contacted and crucial information such as gas envelope size, payload, cost, gondola dimensions were obtained. This information was used in the design of the 4 breadboards such that the combined structure would be able to fit into the actual gondola. The designs were then sent to the PCB Fabrication Lab in NUS and there, the actual PCBs were produced. New components were purchased and soldered onto these PCBs.

Figure 10.1 shows the gondola that was purchased off the shelf and Figure 10.2 shows the gondola that has been fitted with the autonomous flight controls. Appendix 10.1 and 10.2 describe the components in the unmodified and modified gondolas.



Figure 10.1 - Off the shelf Gondola

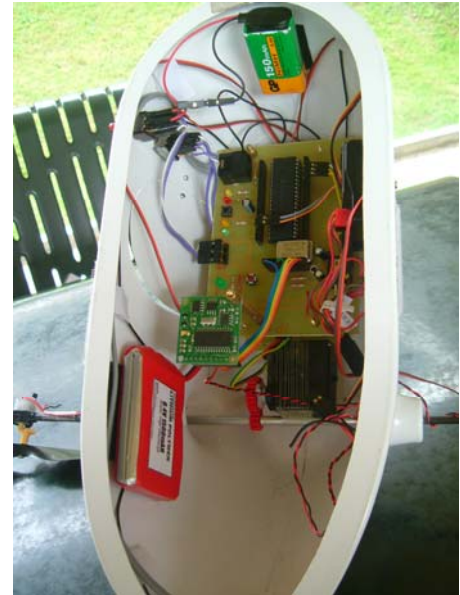


Figure 10.2 - Modified Gondola with autonomous flight controls

Concurrently, the quote was obtained from the supplier and purchase arrangements were made. When the actual airship arrived, the stacked PCBs were mounted into the gondola and taken for outdoor handheld test, which will be explained in greater detail in Chapter 9.2. The connections to the various motors were also modified such that they would be actuated properly by the microcontroller and not the remote control receiver.

11. Flight Tests

With the completion of the design, building and verification of the trolley system for autonomous flight, the next objectives were then to fit it on the actual flight system, verify it and make appropriate changes if necessary. As the airship was to be an autonomous platform utilizing GPS, it had to be verified outdoors where there was a clear line of sight to the various GPS satellites. Furthermore, as the flight system is susceptible to wind conditions, the flight tests were done in the pre-dawn to dawn period where the wind was usually at a minimum and there was sufficient sunlight to be able to capture the flight process on film. The location chosen was in the NUS tennis court, where it would be easier to transport the 8 foot long blimp to and where there were wind-breaks lining the fencing of the tennis courts. Figure 11.1 shows how the blimp was transported between the laboratory and the test site. Figure 11.2 is the blimp at the tennis courts.



Figure 11.1- Transporting the Blimp



Figure 11.2 - Blimp at NUS tennis courts

Initially, the first flight tests conducted were hand-held gondola tests. In the mode of testing, the user simulated the flight platform and carried the gondola around, facing the gondola and moving as indicated by the motors.

With the successful completion of these hand held tests, the next step was then to fit the actual gondola onto the airship and let it navigate and survey autonomously. With the tests on the airship, wind effects on the system were noted. More importantly, drift of the airship sideways when performing bearing correction was noted. This was because the integrated thrust motors and rudder motor method of propulsion as explained in Chapter 5.1 was used.

After analyzing the problem at hand, the independent, bi-directional, variable-speed thrust motors method of propulsion explained in Chapter 5.2 was designed and implemented. This eliminated the drift and cumulated in the successful autonomous navigation of the flight system, meeting the objectives of this project. Figures 11.3 to 11.7 show the blimp navigation autonomously towards a waypoint marked by balloons, while Figures 11.8 to 11.12 show the view from the onboard surveillance camera.



Figure 11.3- Initial bearing Correction



Figure 11.4- Flying towards waypoint



Figure 11.5- Blimp on its way to waypoint



Figure 11.6 – Blimp very close to waypoint



Figure 11.7 – Blimp hits waypoint head on



Figure 11.8 – Starting view



Figure 11.9 – Blimp still some way off



Figure 11.10 – Blimp heading closer



Figure 11.11 – Blimp very close to waypoint



Figure 11.12 – Blimp hits target

11. Evaluation of Autonomous Airship

The airship is viable as an autonomous surveillance platform. As compared to other types of platforms, it is capable of extended periods of stationary surveillance as the lift used is provided by the difference in density between helium and air.

As an autonomous platform, it does not need a human to control its actions and is able to determine which bearing to head towards to, which a human operator might find hard to do in the absence of landmarks. Thus, manpower resources can be maximized as only 1 operator is needed to enter waypoints for a number of blimps and monitor the video images sent back.

The specifications of the current flight platform developed as follows:

- Autonomous functions – Flight Navigation and Surveillance
- Maximum Waypoints – 50
- Maximum Cruise Speed – 1.5ms^{-1}
- Maximum rate of turn (Stationary) – 2.5 rpm
- Rise time 0 to 100 degrees – 15.5 seconds
- Maximum Operating Conditions – Maximum wind speed of 1.5ms^{-1}
- Payload of system – 800g
- Cost of Autonomous Controls – Less than S\$400 (excluding cost of fabricating PCBs)

13. Recommendations

What has been achieved in this project is a proof of concept of an autonomous flight platform, and in this case a blimp has been chosen. Further improvements to the current flight system to enable it to operate in a military operational setting would be:

- Wind counter measures – one of the main concerns in the employment of a blimp for military operations is the effect of wind of the blimp. Therefore, wind counter measures, in choice of system design, choice of motor, propeller, sensors and any algorithm, should be studied and implemented. Also, this would allow the blimp to perform stationary surveillance in the presence of wind.
- Proximity sensors and gyroscopes– Proximity sensors can be mounted onto the airship such that it can perform obstacle avoidance and perform smooth landing. Gyroscopes can be used to maintain pitch and roll stability.
- Improved surveillance system – the inclusion of a camera system which has a longer transmission range and is able to pan, tilt, zoom and auto-focus autonomously would improve the quality of the video images sent back, which increases the effectiveness of the deployment of an airship. Studying the lens mechanism in a digital camera or video camera might provide some good clues.
- Vision recognition – A computer algorithm that allows the tracking and surveillance of a particular.
- Route mapping – An algorithm that is able to find the equation to the best fit curve among the waypoints. In this way, intermediate waypoints can be generated with only a small amount of RAM, ensuring a closer adherence to the desired flight path for a minimum amount of resources.

14. Conclusion

In conclusion, a proof of concept autonomous flight platform was developed and produced at the end of this project, meeting the objectives of this project as set forth by the project sponsor, HQ Combat Engineers.

An 8 foot (2.4) blimp Remote Control blimp was purchased and the controls were extensively modified. A literature survey revealed that although there is some research being done on autonomous blimps, with the 2 notable projects being AURORA and LAAS_CNRS, the smallest autonomous blimp thus far is at least 8m in length. Thus this project is innovative in the sense of developing an autonomous flight navigation and surveillance system in-house, under tight payload constraints of a net payload of 800g.

Electronic controls for the purpose of autonomous flight navigation and surveillance, consisting of 4 Printed Circuit Boards, with a microcontroller at its core, were designed and built. These 4 PCBs are built by function, and they are the Central Processing Board (CPU), the RS232 Board, the Motor Drive Board and the GPS Receiver Board. 4 different Integrated Circuits and a GPS receiver were used to accomplish this function. The control system was developed for a cost of less than \$400, in comparison to the current market offer, Micropilot™, which costs \$8000.

Modifications were done to the mechanical actuation system that came with the Remote Control blimp. The current system, based on a rudder, was analyzed to be incapable of performing stationary yaw control. Therefore, a new method was developed to replace

this method of control. The 2 thrust motors were made independent, variable speed, bi-directional. Experiments were done to obtain the maximum rate of stationary turning (yaw) is 2.5 rpm.

Also, a proportional control was developed for stationary yaw control. Experiments were carried out to quantify the effectiveness of the controller. The rise time was found to be 15.5 seconds for a 100° change. Proportional controllers were also developed for navigational yaw control and thrust motor control. The transfer function for yaw control was also determined experimentally, where the response to a step input was used. The transfer function is:

$$T(s) = \frac{\theta(s)}{V(s)} = \frac{100 \times (12.6823s + 45.68127s^2 + 66.66233s^3 + 13.46875s^4 - 13.4969s^5 - 3.26738s^6)}{s^4 + 1.1216s^5 + 0.001213s^6 - 0.22705s^7 - 0.02893s^8}$$

The source code was developed entirely as part of this project. The source code allows for authentication, autonomous navigation of up to 50 waypoints and stationary surveillance at predetermined points. Programming was done in “C” language, which was chosen because it offered high level control among the low level languages.

Experiments were carried out to determine propeller thrust force for various speeds, in both the forward and reverse directions. This information was essential to the development of the stationary yaw control. Additionally, experiments were also carried out to determine the effects of wind force. The flight platform was determined to have a Coefficient of Drag, C_D , of 0.26, which is between that of a sphere (0.39) and a streamline body (0.05).

An equation for the maximum operating conditions for this flight platform was also developed, and used to determine that the maximum wind force the current system can function at is 1.5ms^{-1} . A general equation was also developed for systems which are dynamically similar.



The project culminated in successful field tests, with both the airship performing reconnaissance while navigating autonomously.

Through the duration of this project, design skills, technical abilities, programming skills, experimental setup and analysis of results knowledge were demonstrated across multiple disciplines: mechanical engineering, electronic engineering and software programming.

References

Books

1. Tsui, James Bao-yen. “Fundamentals of Global Positioning System Receivers: A Software Approach”, John Wiley & Sons, Inc, 2000
2. Joseph B. Franzini E, and John Finnemore. “Fluid Mechanics” 9th Edition, McGraw Hill, 1997
3. Gene H. Hostetter, Clement J. Savant, Jr. , and Raymond T. Stefani. “Design of Feedback Control Systems”, Saunders College Publishing 1989
4. Douglas A. Cassell. “Microcomputers & Modern Control Engineering”, Reston Publishing Company, Inc, 1983
5. Christopher T. Kilian. “Modern Control Technology, Components and Systems”, West Publishing Company, 1996

Journal Articles

6. Josué Jr. G. Ramos, et al. “A Software Environment for an Autonomous Unmanned Airship” IEEE International Conference on Advanced Intelligent Mechatronics, Sep 1999.
7. Sergio B. Varella Gomes, and Josué Jr. G. Ramos. “Airship Dynamic Modeling for Autonomous Operation”, IEEE International Conference on Robotics & Automation, May 1998
8. Guoqing Xia, and Dan R. Corbett. “Cooperative Control Systems of Searching Targets Using Unmanned Blimps”, 5th World Congress on Intelligent Control and Automation, June 2004

9. Josué Jr. G. Ramos, et al. “Development of a VRML/Java Unmanned Airship Simulating Environment”, IEEE International Conference on Intelligent Robots and Systems, 1999
10. Emmanuel Hygounenc, and Philippe Souères. “Lateral path following GPS-based control of a small-sized unmanned blimp”, IEEE International Conference on Robotics & Automation, Sep 2003
11. José Raul Azinheira, et al. “Mission Path Following for an Autonomous Unmanned Airship”, International Conference on Robotics & Automation, Apr 2000.
12. Sullivan, Arthur, and Turner, William. “Eye in the sky: airship surveillance”, International Telemetering Conference, 1995
13. Emmanuel Hygounenc, et al. “The Autonomous Project of LAAS-CNRS: Achievements in Flight Control and Terrain Mapping”, International Journal of Robotics Research, Vol 23, No. 4-5, April-May 2004

Datasheets and Technical Manuals

14. American Blimp Corporation. “Airships: An Ideal Platform For Human or Remote Sensing in the Marine Environment” 2000
15. Trimble Navigation Limited. “Lassen™ SQ GPS Receiver. System Designer Reference Manual.” Revision A, June 2002
16. Microchip Technology Incorporated. “PIC 18FXX2 Data Sheet. High Performance, Enhanced FLASH, Microcontrollers with 10-Bit A/D” 2002

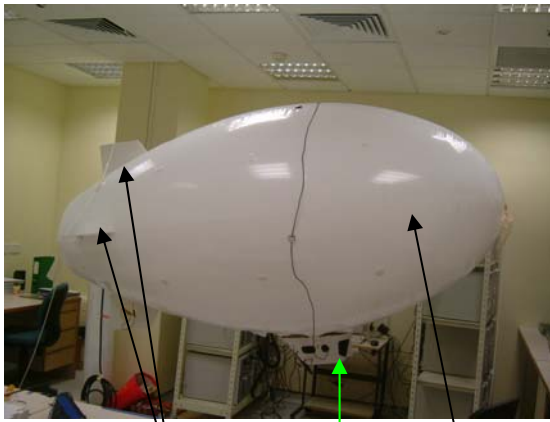
17. Microchip Technology Incorporated. “PIC 16F87X Data Sheet. 28/40 Pin 8-Bit CMOS FLASH Microcontrollers” 2001
18. Maxim Integrated Products. “MAXIM +5V-Powered, Multichannel RS-232 Drivers/Receivers” Revision 14, Aug 2004
19. SGS-Thomson Microelectronics “L293D-L293DD. Push-Pull Four Channel Driver with Diodes” June 1996
20. Fairchild Semiconductor. “MC78XX/LM78XX/MC78XXA. 3-Terminal 1A Positive Voltage Regulator” Revision 1.0.1, 2001
21. National Semiconductor Corporation. “LMS 1585A/LMS 1587. 5A and 3A Low Dropout Fast Response Regulators” 2000

Websites

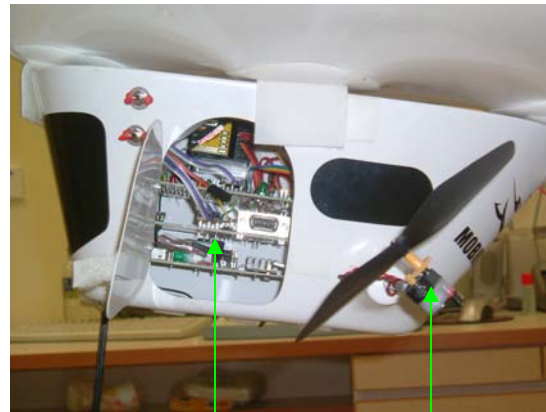
22. Boeing .”ScanEagle UAV”
<<http://www.boeing.com/defense-space/military/unmanned/scaneagle.html>>
23. Trimble Navigation Limited. “GPS Tutorial” Sep 2005
< <http://www.trimble.com/gps/>>
24. Leroy Davis “Logic Threshold Voltage Levels” Jan 2005
< http://www.interfacebus.com/voltage_threshold.html>
25. Lammert Bies. “RS-232 Specifications and Standard” Nov 2005
< http://www.lammertbies.nl/comm/info/RS-232_specs.html>
26. Custom Computer Services “User Forum – General CCS C Discussion”
< <http://www.ccsinfo.com/forum/>>

Appendix 2.1

Picture of Blimp and Control System



Tail Fin Stabilizers Gondola Gas Envelope



Control Hardware Actuators

Appendix 3.1

NMEA Field Definitions

Many of the NMEA data fields are of variable length, and the user should always use the comma delineators to parse the NMEA message data field. Table C.2 specifies the definitions of all field types in the NMEA messages supported by Trimble.

Table C.2 Field Type Summary

Type Symbol Definition

Status A Single character field:

A=Yes, data valid, warning flag clear

V=No, data invalid, warning flag set

Special Format Fields

Latitude IIII.III Fixed/variable length field:

Degreesminutes.decimal-2 fixed digits of degrees, 2 fixed digits of minutes and a variable number of digits for decimal-fraction of minutes. Leading zeros always included for degrees and minutes to maintain fixed length. The decimal point and associated decimal-fraction are optional if full resolution is not required.

Longitude yyyyy.yyy Fixed/Variable length field:

Degreesminutes.decimal-3 fixed digits of degrees, 2 fixed digits of minutes and a variable number of digits for decimal-fraction of minutes. Leading zeros always included for degrees and minutes to maintain fixed length. The decimal point and associated decimal-fraction are optional if full resolution is not required.

Time hhmmss.ss Fixed/Variable length field: hoursminutesseconds.decimal-2 fixed digits of minutes, 2 fixed digits of seconds and a variable number of digits for decimal-fraction of seconds. Leading zeros always included for hours, minutes, and seconds to maintain fixed length. The decimal point and associated decimal-fraction are optional if full resolution is not required.

Note – Spaces are only be used in variable text fields.

Note 2 – Units of measure fields are appropriate characters from the Symbol column (see Table C.2), unless a specified unit of measure is indicated.

Note 3 – Fixed length field definitions show the actual number of characters. For example, a field defined to have a fixed length of 5 HEX characters is represented as hhhhh between delimiters in a sentence definition.

Defined Some fields are specified to contain pre-defined constants, most often alpha characters. Such a field is indicated in this standard by the presence of one or more valid characters. Excluded from the list of allowable characters are the following that are used to indicated field types within this standard:

“A”, “a”, “c”, “hh”, “hhmmss.ss”, “llll.ll”, “x”, “yyyy.yy”

Numeric Value Fields

Variable x.x Variable length integer or floating numeric field. Optional leading and trailing zeros. The decimal point and associated decimal-fraction are optional if full resolution is not required (example: 73.10=73.1=073.1=73).

Fixed HEX hh Fixed length HEX numbers only, MSB on the left

Information Fields

Fixed Alpha aa Fixed length field of upper-case or lower-case alpha characters

Fixed number xx Fixed length field of numeric characters

Appendix 3.2

NMEA 0183 GPGGA Message Format

GGA - GPS Fix Data

The GGA message includes time, position and fix related data for the GPS receiver.

```
$GPGGA,hhmmss.ss,llll.llll,a,nnnnn.nnn,b,t,uu,v.v,w.w,M,x.x,M,y.y,zzzz*hh <CR><LF>
```

Table C.4 GGA - GPS Fix Data Message Parameters

Field # Description

1 UTC of Position

2,3 Latitude, N (North) or S (South)

4,5 Longitude, E (East) or W (West)

6 GPS Quality Indicator: 0 = No GPS, 1 = GPS, 2 = DGPS

7 Number of Satellites in Use

8 Horizontal Dilution of Precision (HDOP)

9, 10 Antenna Altitude in Meters, M = Meters

11, 12 Geoidal Separation in Meters, M=Meters. Geoidal separation is the difference between the WGS-84 earth ellipsoid and mean-sea-level.

13 Age of Differential GPS Data. Time in seconds since the last Type 1 or 9 Update

14 Differential Reference Station ID (0000 to 1023)

hh Checksum

Appendix 3.3

Relative Weighing Factor Chart

Methodology: 2 properties are compared. A “1” is assigned to the Property that is deemed to be relatively more important, and “0” for the other. All combinations are considered. The relative weighing factor is determined by the relative number of “1”s a property has.

Property\ Comparison	(1) & (2)	(1) & (3)	(1) & (4)	(1) & (5)	(1) & (6)	(2) & (3)	(2) & (4)
1. Weight	1	0	0	1	1		
2. Battery Voltage	0					0	0
3. Accuracy		1				1	
4. Customer Support			1				1
5. Size				0			
6. Cost					0		

Property\ Comparison	(2) & (5)	(2) & (6)	(3) & (4)	(3) & (5)	(3) & (6)	(4) & (5)	(4) & (6)
1. Weight							
2. Battery Voltage	1	0					
3. Accuracy			0	1	1		
4. Customer Support			1			1	1
5. Size	0			0		0	
6. Cost		1			0		0

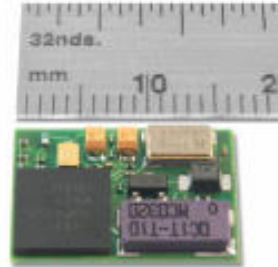
Property\ Comparison	(5) & (6)	Number of “1”s	Weighting Factor, W_i
1. Weight		3	$W_1 = 3/15$
2. Battery Voltage		1	$W_2 = 1/15$
3. Accuracy		4	$W_3 = 4/15$
4. Customer Support		5	$W_4 = 5/15$
5. Size	1	1	$W_5 = 1/15$
6. Cost	0	1	$W_6 = 1/15$

Appendix 3.4

GPS Modules Sourced



Trimble Lassen SQ



Motorola FS Oncore



Garmin GPS 35 TracPak



Laipac TF30 Evaluation Kit



Parvus Orbitrak 8 R



San Hose DGPS -220-PC

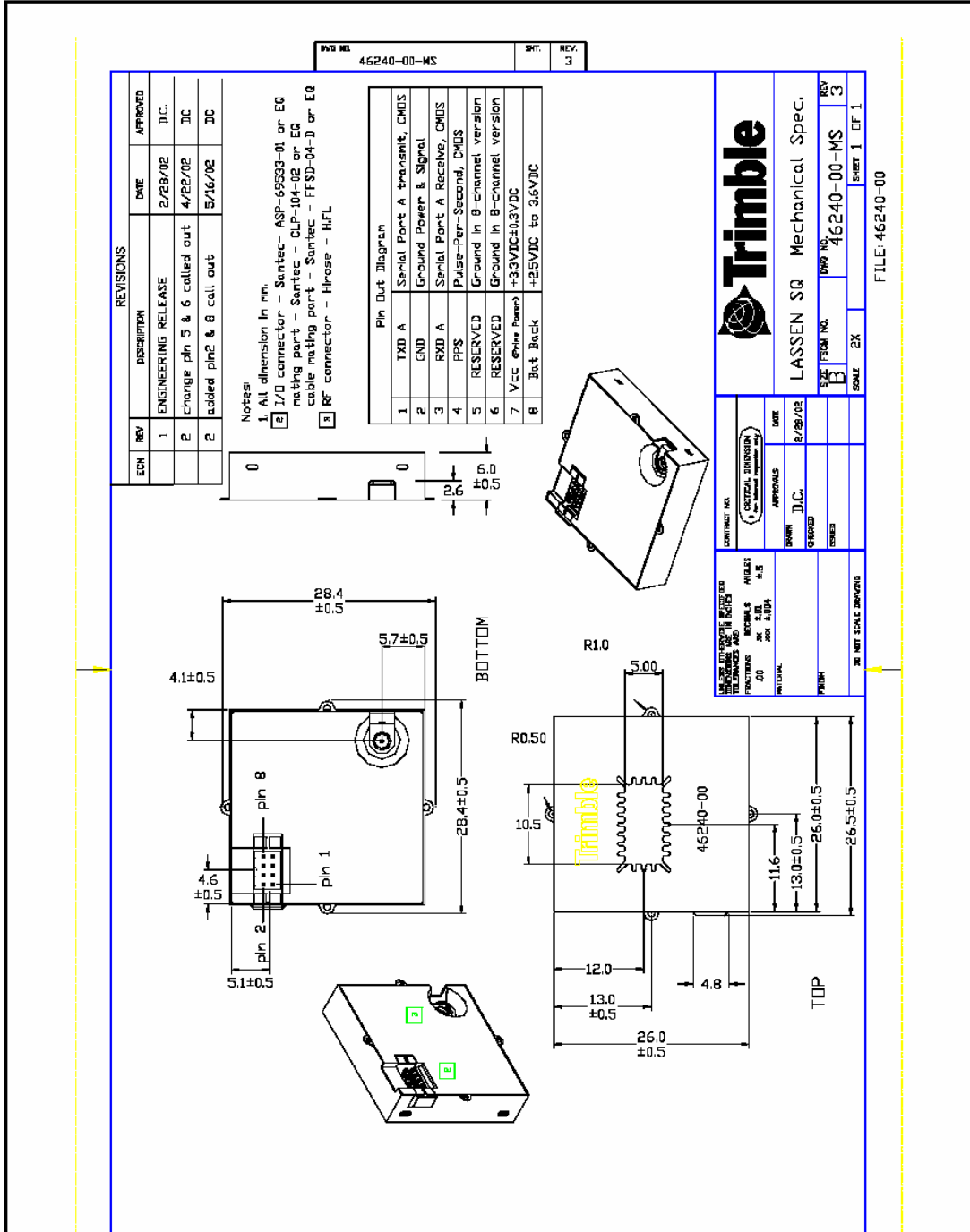
Appendix 3.5

Go/No Go & Weighted Property Index Chart

GPS Module	Go/ No-Go Screening		Customer Support, 5/15	Accuracy, 4/15	Weight, 3/15	Voltage 1/15	Size 1/15	Cost, 1/15	Module Performance Index, γ
	Weight	Cost							
Trimble	S	S	100	100	80	100	100	100	96
Motorola	S	S	20	100	100	100	100	100	73.3
Garmin	S	S	30	50	90	25	50	50	49.7
Laipac	?	US	-	-	-	-	-	-	-
Parvus	?	US	-	-	-	-	-	-	-
San Hose	US	?	-	-	-	-	-	-	-

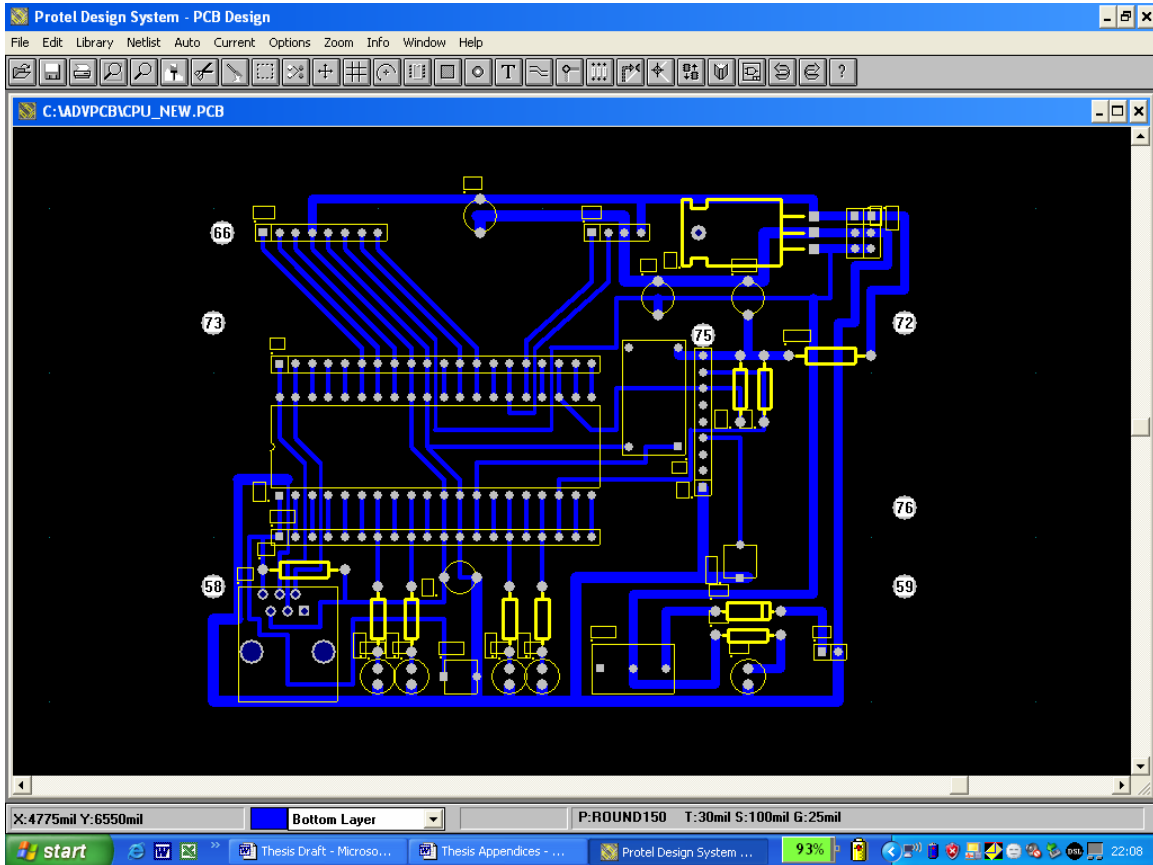
Appendix 3.6

Technical Drawing of Trimble Lassen GPS Receiver



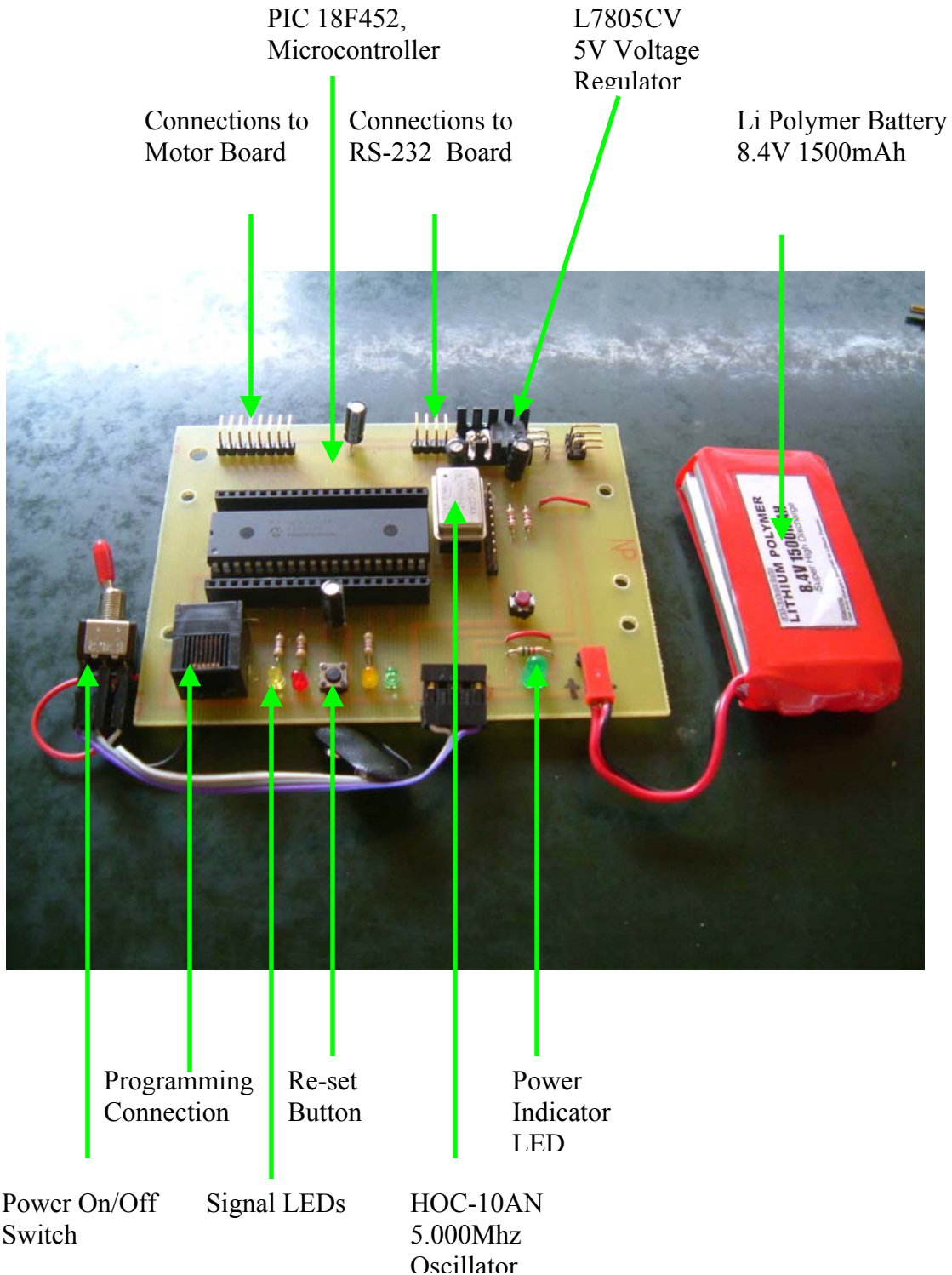
Appendix 4.1

Protel Design of CPU PCB



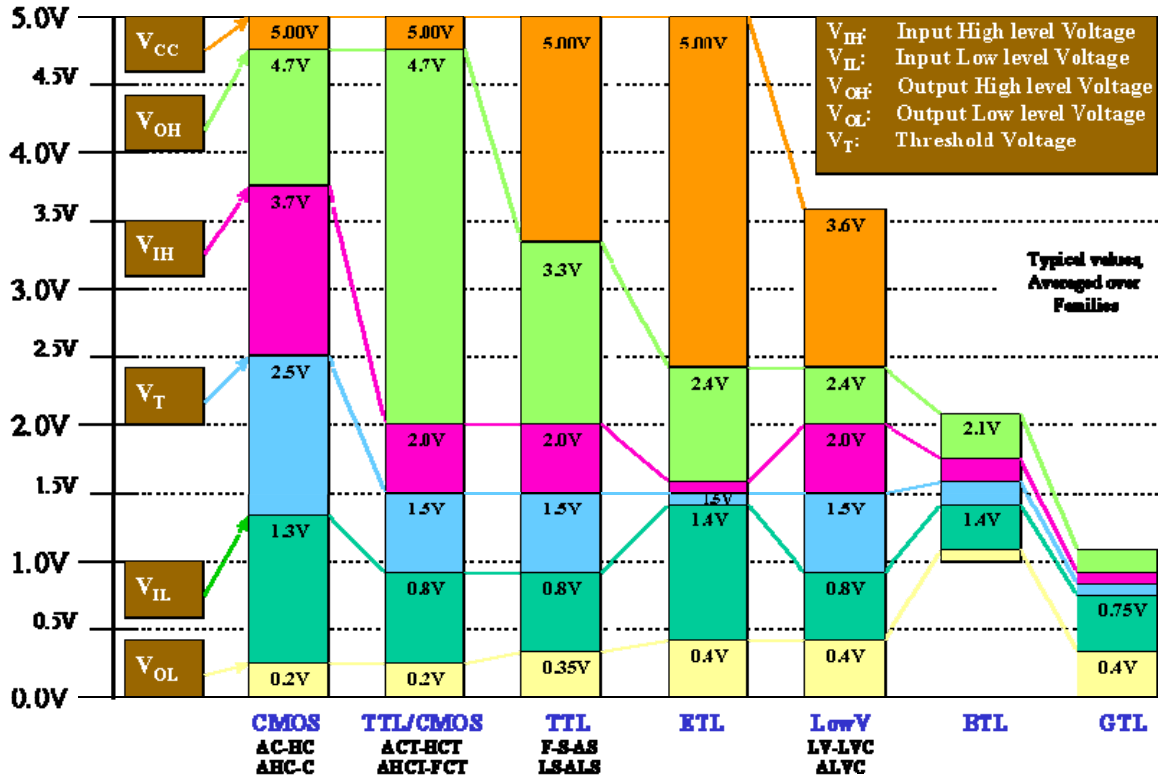
Appendix 4.2

Components in CPU PCB



Appendix 4.3

Graph of the Different Logic Formats



Terms

V_{CC} : The voltage applied to the power pin(s). In most cases the voltage the device needs to operate at.

V_{IH} : [Voltage Input High] The minimum positive voltage applied to the input which will be accepted by the device as a logic high.

V_{IL} : [Voltage Input Low] The maximum positive voltage applied to the input which will be accepted by the device as a logic low.

V_{OL} : [Voltage Output Low] The maximum positive voltage from an output which the device considers will be accepted as the maximum positive low level.

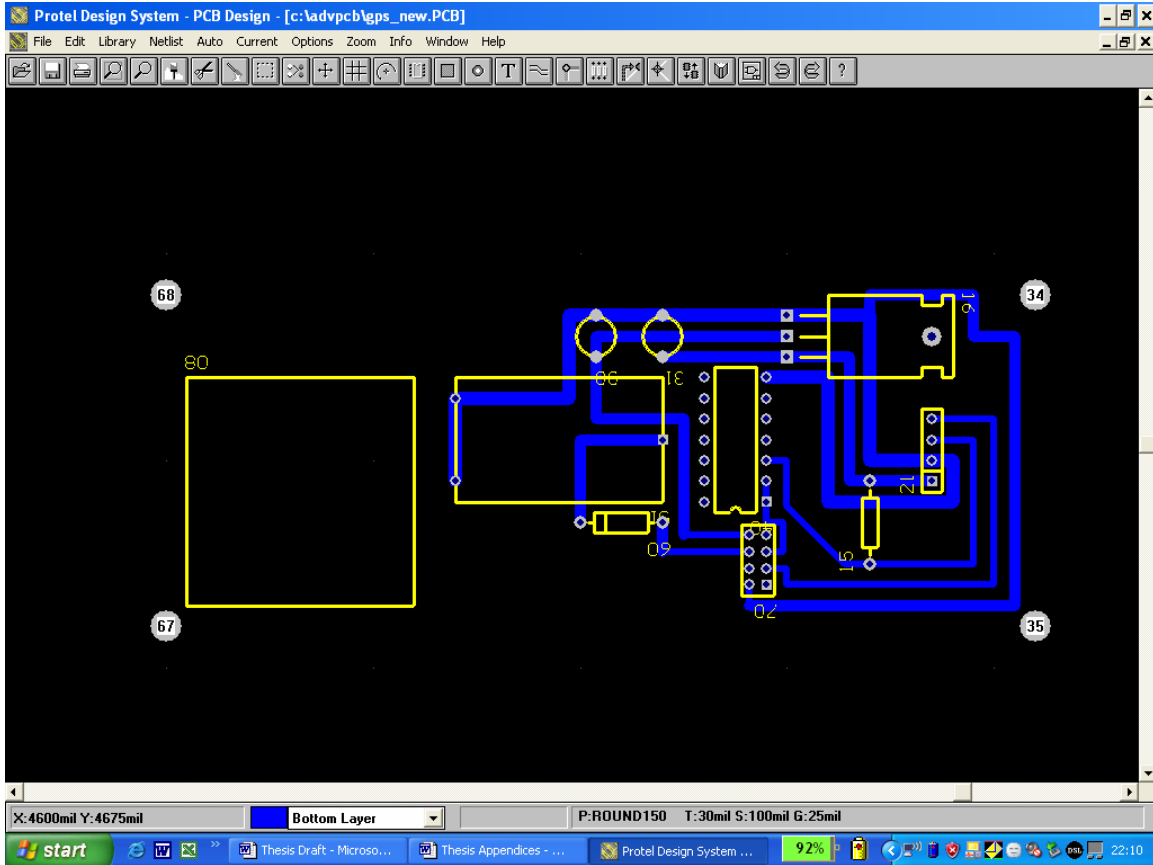
V_{OH} : [Voltage Output High] The maximum positive voltage from an output which the device considers will be accepted as the minimum positive high level.

V_T : [Threshold Voltage] The voltage applied to a device which is "transition-Operated", which cause the device to switch. May also be listed as a '+' or '-' value.

Source: http://www.interfacebus.com/voltage_threshold.html

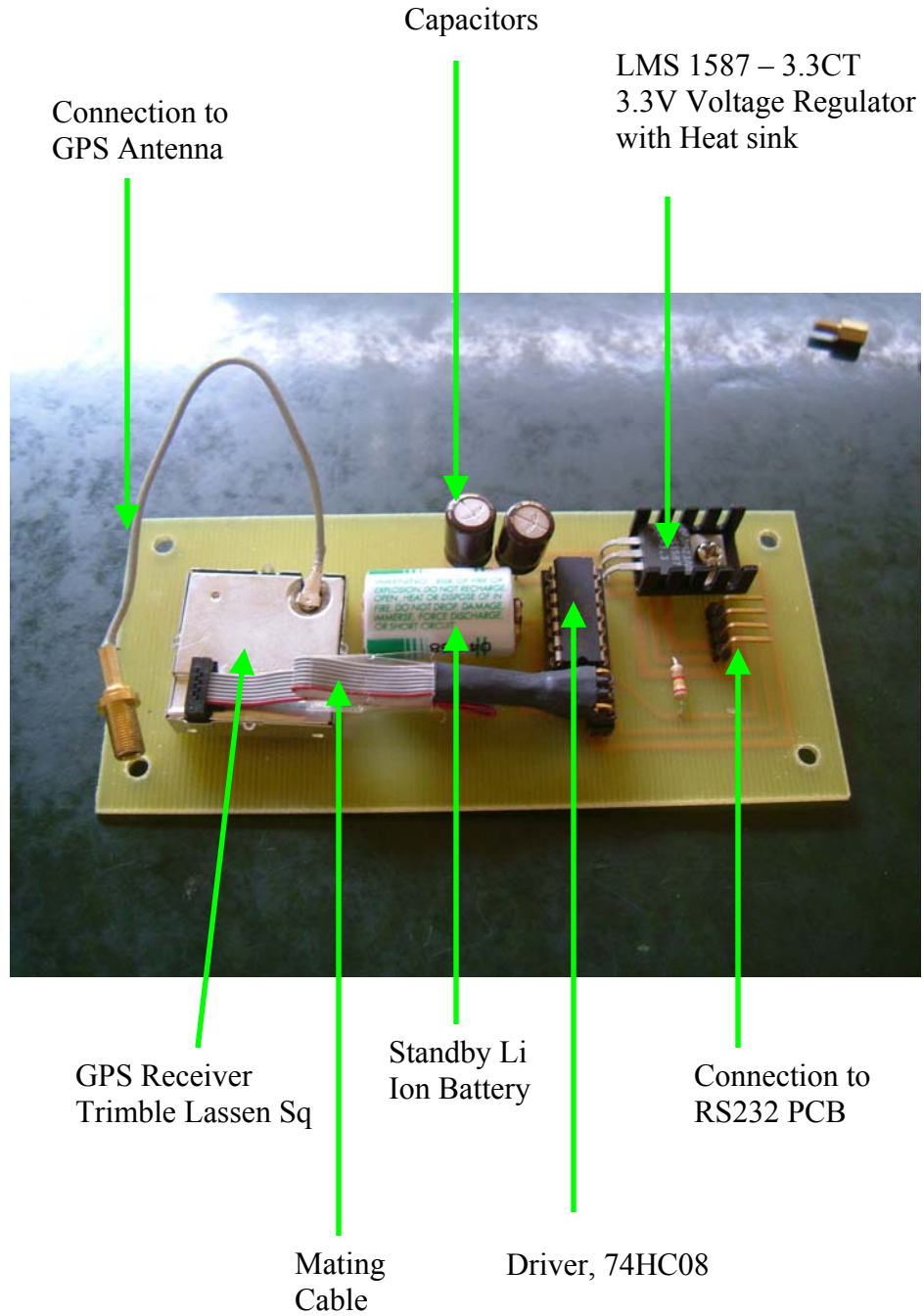
Appendix 4.4

Protel Design of GPS Receiver PCB



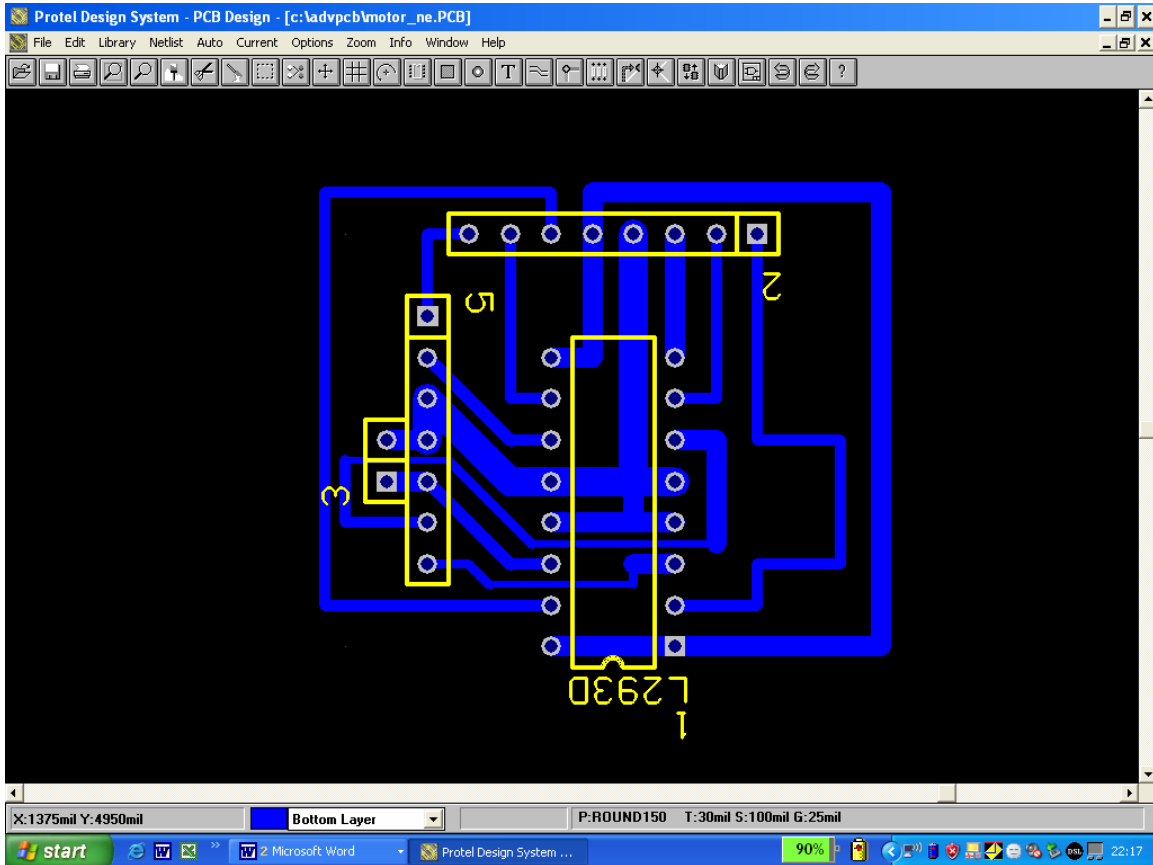
Appendix 4.5

Components in GPS Receiver PCB



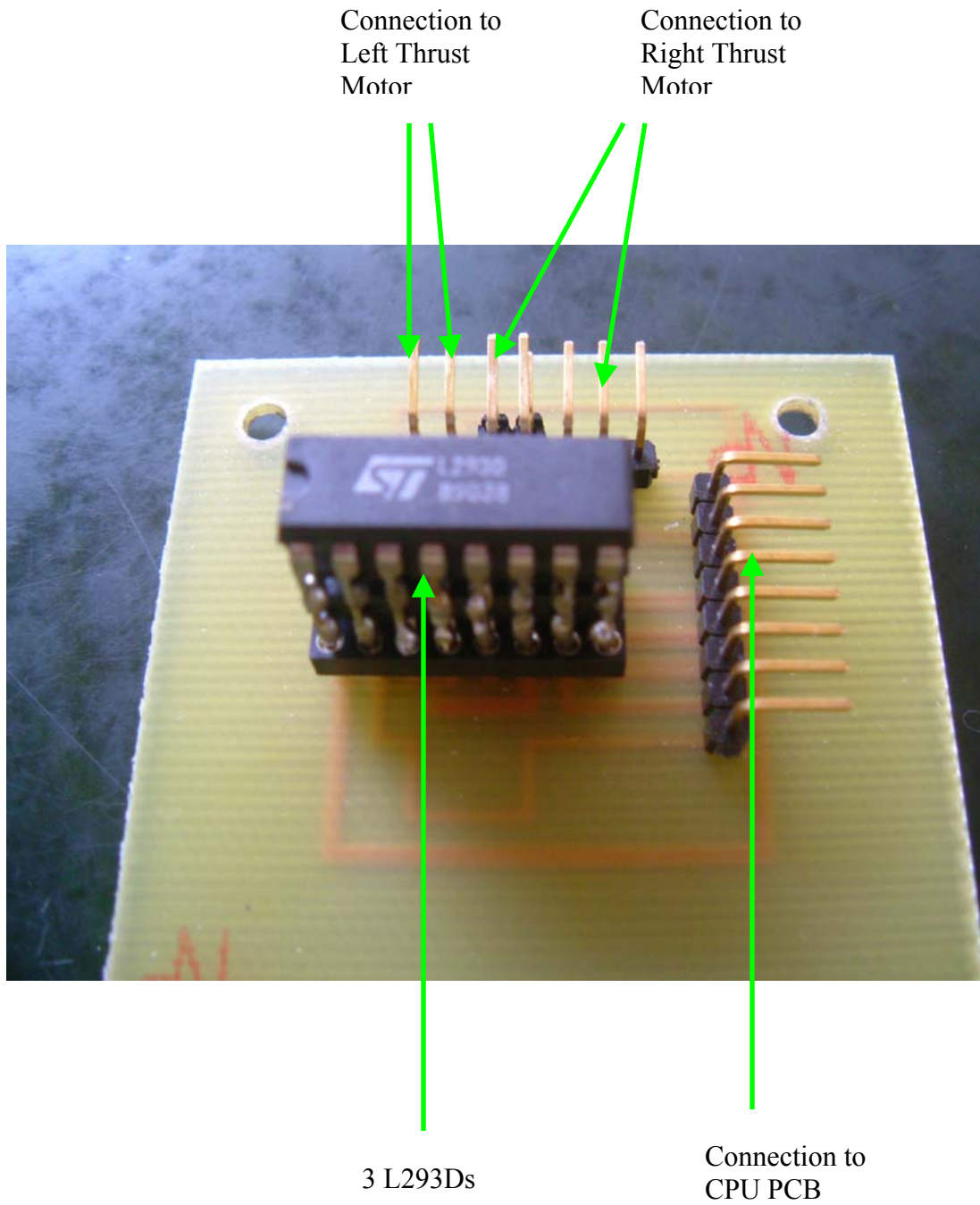
Appendix 4.6

Protel Design of Motor Drive PCB



Appendix 4.7

Components in Motor Drive PCB



Appendix 4.8

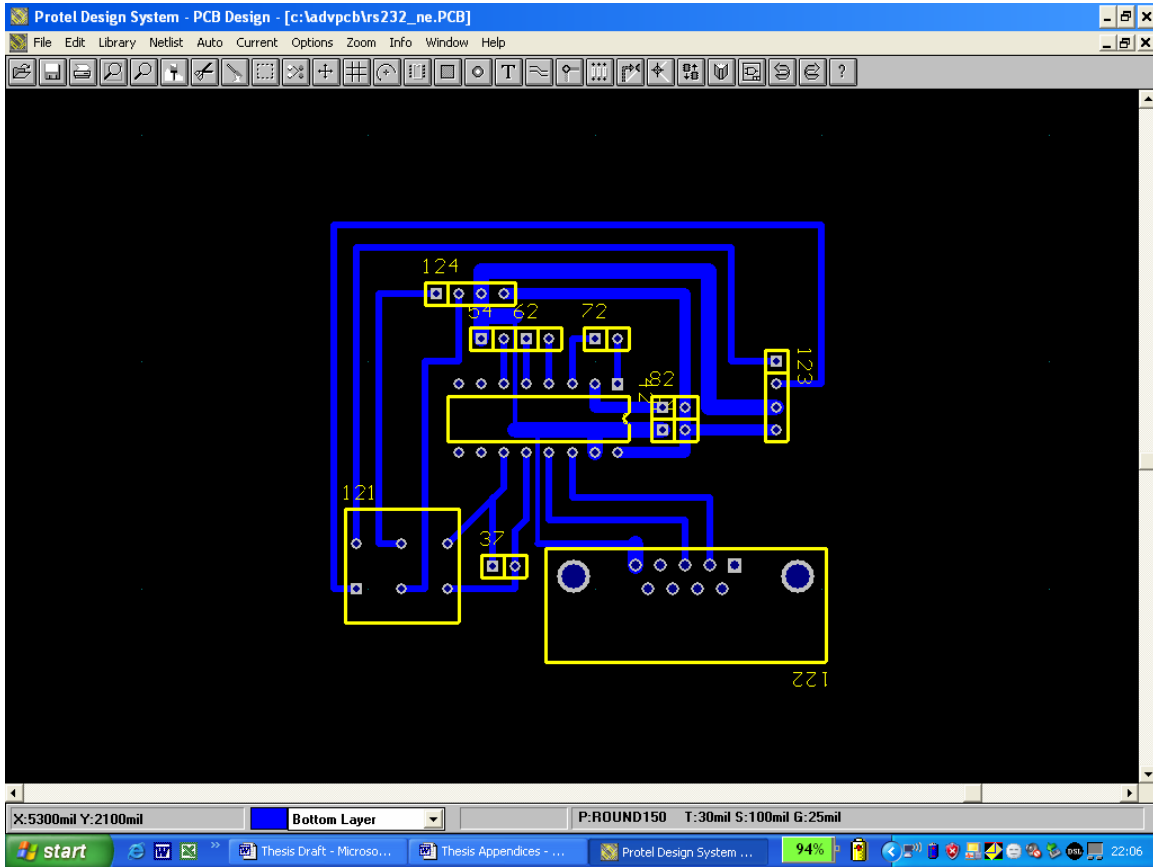
RS 232 Voltage Levels

RS232 voltage values		
Level	Transmitter capable (V)	Receiver capable (V)
Space state (0)	+5 ... +15	+3 ... +25
Mark state (1)	-5 ... -15	-3 ... -25

Source: http://www.lammertbies.nl/comm/info/RS-232_specs.html

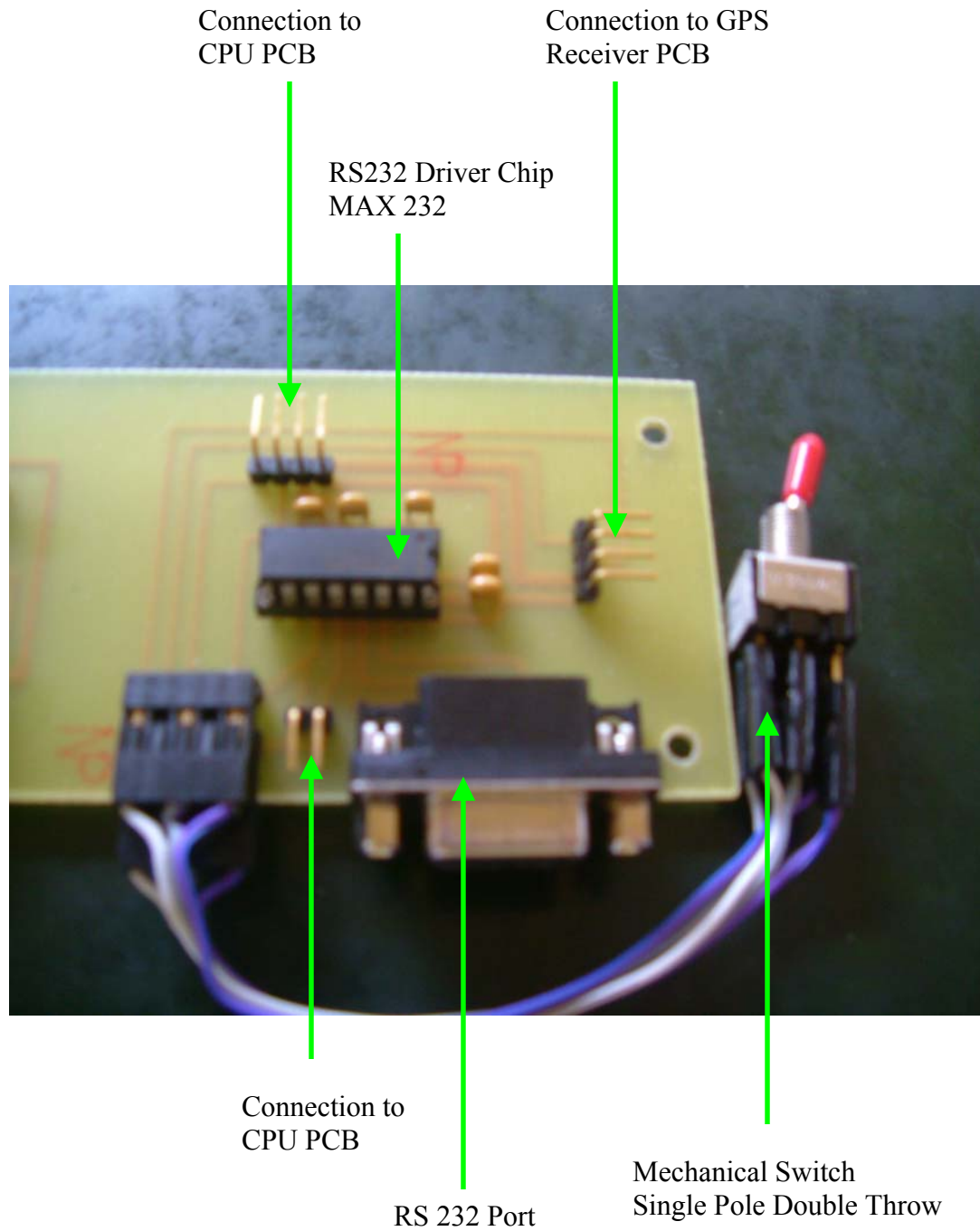
Appendix 4.9

Protel Design of RS 232 PCB



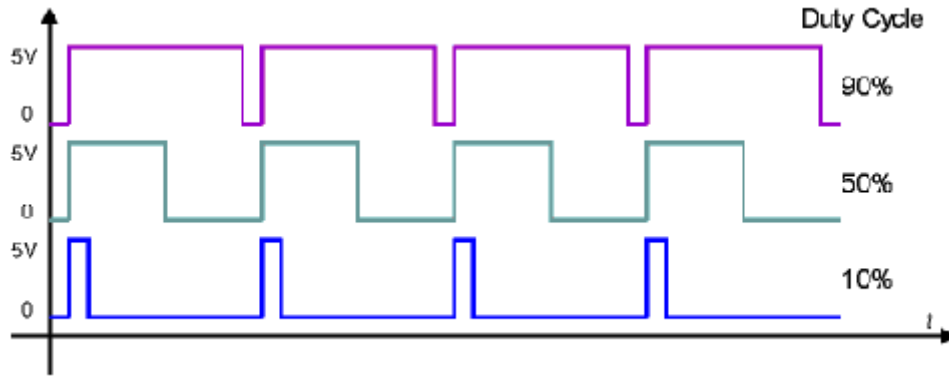
Appendix 4.10

Components of RS 232 PCB



Appendix 5.1

Duty Cycle Concept



Source: <http://www.isk.kth.se/kursinfo/mekatronik/9899/grupper/g1/teknisk.html>

Appendix 6.1

Code for “Lighting LEDs with timing control”

Please contact author for source code!

Appendix 6.2

Code for “Serial Transmit and Receive”

Please contact author for source code!

Appendix 6.3

Code for “Servo and DC Motor Control”

Please contact author for source code!

Please contact author for source code!

Appendix 6.4

Code for “Variable DC Motor Speed and Direction Control”

Please contact author for source code!

}

Please contact author for source code!

Please contact author for source code!

Appendix 6.5

Code for “Bearing reading from electronic compass”

Please contact author for source code!

Please contact author for source code!

Appendix 6.6

Code for “Reading GPS coordinate outputs from GPS
receiver”

Please contact author for source code!

Appendix 6.7

Source Code

Please contact author for source code!

Please contact author for source code!

Please contact author for source code!

Please contact author for source code!

Please contact author for source code!

Please contact author for source code!

Please contact author for source code!

Please contact author for source code!

Please contact author for source code!

Please contact author for source code!

Please contact author for source code!

Please contact author for source code!

Please contact author for source code!

Please contact author for source code!

Please contact author for source code!

Please contact author for source code!

Appendix 7.1

Resolution capabilities of the wireless camera system

Acrobat Reader - [Previous Thesis.pdf]

File Edit Document View Window Help

Table 4A: Experimental data of image resolution

Flight Altitude (m)	4.500	9.000	13.500	18.000	22.500
Range (m)	14.705	16.643	19.449	22.804	26.500
Original dimension (m)	Dimension of object on LCD screen (m)				
	Resolution = 320 x 240 ppi				
0.100	0	0	0	0	0
0.200	0.002	0.001	0.0005	0	0
0.300	0.003	0.002	0.001	0.0005	0
0.400	0.004	0.003	0.002	0.001	0.0005
0.500	0.005	0.004	0.003	0.002	0.001
0.600	0.006	0.005	0.004	0.003	0.002
0.700	0.007	0.006	0.005	0.004	0.003
0.800	0.008	0.007	0.006	0.005	0.004
0.900	0.009	0.008	0.007	0.006	0.005

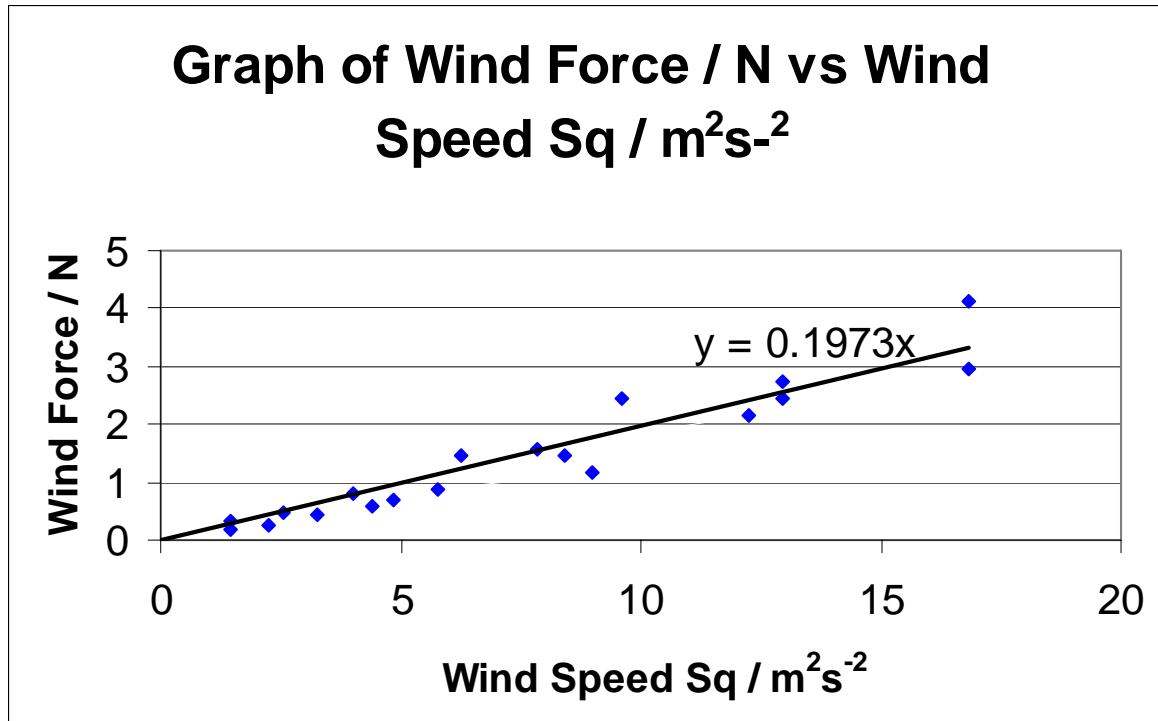
165% 41 of 75 8.26 x 11.69 in

start Thesis Draft for 5... Thesis Appendice... FYP Acrobat Reader - ... 02:14

Appendix 8.1

Graph of Wind Force Vs Wind Speed

(Head Wind)



Appendix 8.2

Derivation of C_D

$$F_w = 0.1973V^2$$

$$F_D = \frac{1}{2}C_D\rho_{air}AV^2$$

Under maximum operating condition, the airship is stationary and thus $F_w = F_D$

$$\frac{1}{2}C_D\rho_{air}AV^2 = 0.1973V^2$$

$$\rho_{air} = 1.288 \text{ kgm}^{-3}$$

Also, we have been provided the diameter of the airship by the manufacturer.

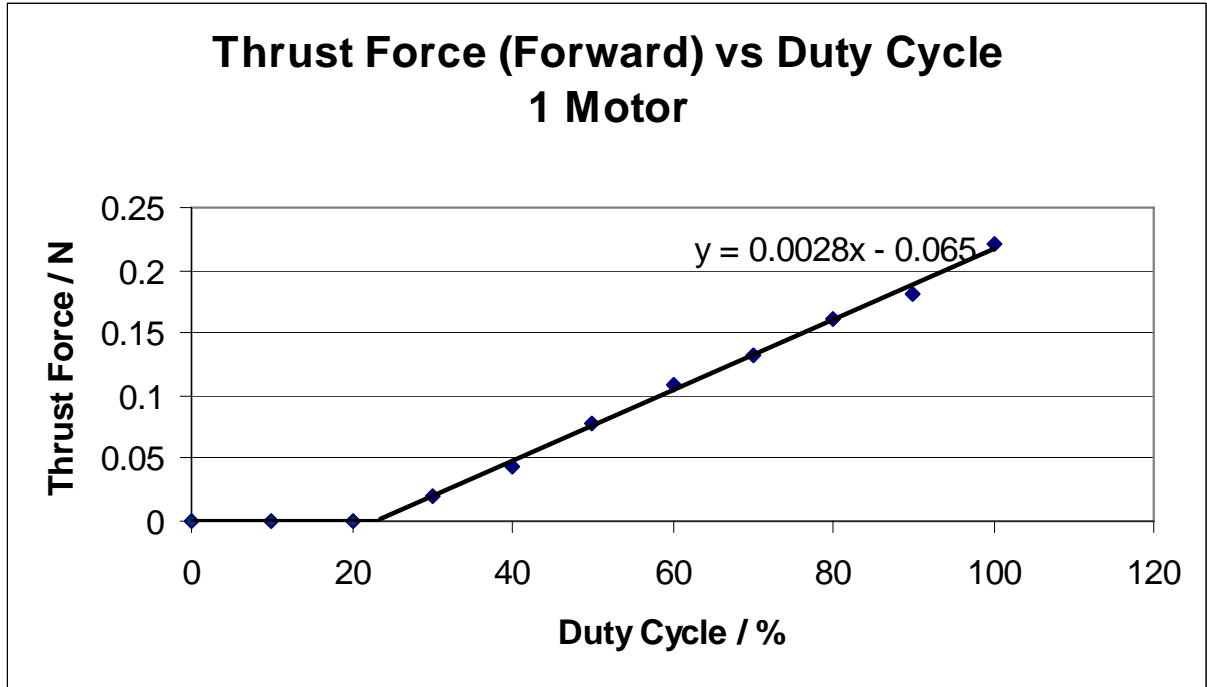
$$A = \frac{\pi}{4}D^2 = \frac{\pi}{4}(1.1938)^2 = 1.1193\text{m}^2$$

$$C_D = \frac{0.1973 \times 2}{1.288 \times 1.1938}$$

$$C_D = 0.26$$

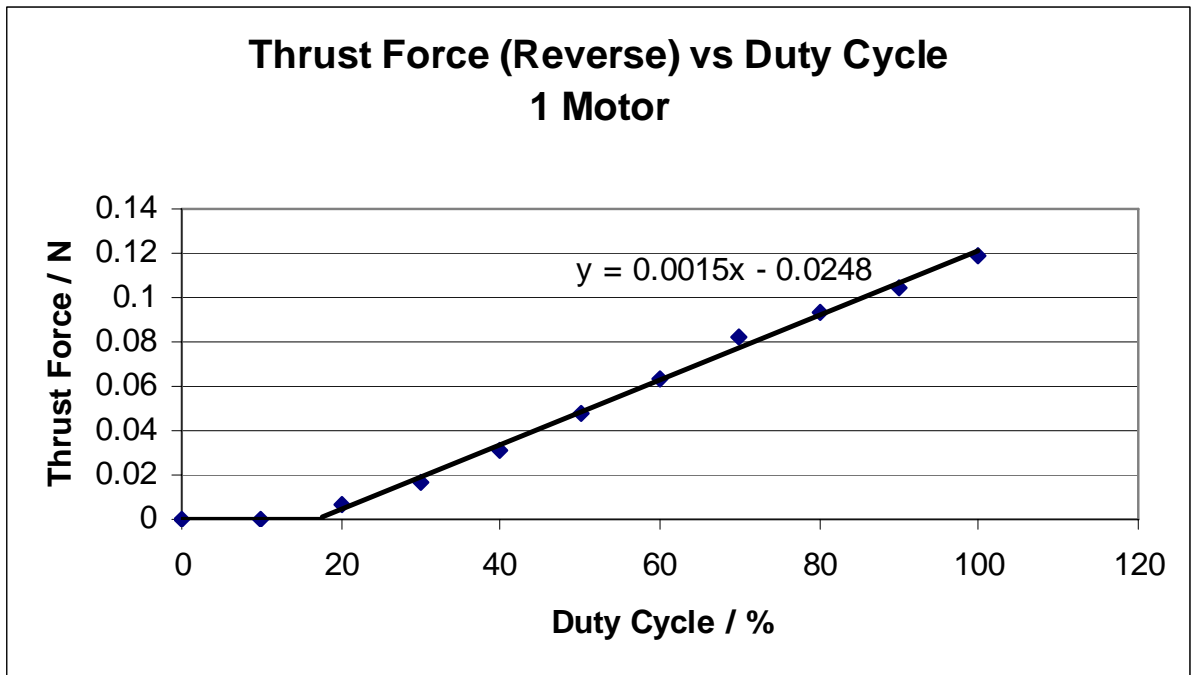
Appendix 8.3

Graph of Thrust Force in the Forward Direction Vs Duty Cycle



Appendix 8.4

Graph of Thrust Force in the Reverse Direction Vs Duty Cycle



Appendix 8.5

Derivation of Equation for Maximum Operating Conditions of Current Platform

For the current platform, the wind force is given by the equation: $F_w = 0.1973V^2$

Thrust force by 1 propeller spinning in the forward direction is given by

$$F_{T,forward} = 0.0028 \times DutyCycle - 0.065$$

Therefore, the maximum Thrust force provided by **Both** propellers is:

$$F_{T,max} = 2 \times (0.0028 \times 100 - 0.065) = 0.43N$$

The maximum operating condition is defined at the point when the force exerted by the wind is equal to the maximum thrust force provided by the thrust motors

$$F_{w,max} = F_{T,max}$$

$$0.1973V_{max}^2 = 0.43$$

$$V_{w,max} = 1.5ms^{-1}$$

Appendix 8.6

Derivation of General Equation for Maximum Operating Conditions

$$F_W = \frac{1}{2} C_D \rho_{air} A V^2 = 0.166 A V^2 \quad \& \quad F_{T,totl} = 2 \times F_{T,max}$$

$$F_W = F_{T,Total}$$

$$0.166 A V_{max}^2 = 2 \times F_{T,max}$$

$$\therefore V_{max} = \sqrt{12.05 \times \frac{F_{T,max}}{A}}$$

Appendix 8.7

Weight of Various Components (Remain the same)

Component Weights

<i>Components which remain the same for Different Sized Airships</i>			
Item	Individual Weight/g	Quantity	Total Weight/g
Gondola with carbon fiber rod and gear	131.83	1	131.83
Wireless Camera with Sponge Padding	26.33	1	26.33
Camera Mounting System	15.14	1	15.14
Wireless Camera Battery, 9V, GP, NiMH, 150mAh, Rechargable	40.81	1	40.81
GPS Receiver PCB	48.65	1	48.65
GPS Antenna, Trimble Magetic Mount Antenna with 1.5m cable, magnets removed	61.4	1	61.4
RS 232 PCB and Motor Drive PCB	48.55	1	48.55
Programming Cable	10.96	1	10.96
Electronic Compass with Mount (2x25mm Spacers)	16.95	1	16.95
CPU PCB	79.19	1	79.19
Spacers, 20mm Brass	2.95	8	23.6
Spacers, 10mm Brass	1.58	4	6.32
Servo Motor with Balsa Wood stand	51.71	1	51.71
Subtotal			561.44

Appendix 8.8

Weight of Various Components (Changes and Optional)

Components which change for Different Sized Airships			
Item	Individual Weight/g	Quantity	Total Weight/g
Tail Fin Stabilizers	32.44	4	129.76
Li Polymer Battery, SHS-Kokam, 2 Cell, 8.4V, 1500mAh, Super High Discharge, Rechargeable	70.45	1	70.45
6 inch Propeller with spindle and 42 tooth gear	3.87	2	7.74
Motor with holder and 10tooth gear	7.68	2	15.36
Gas Bag - 8 foot blimp	500	1	500
Subtotal			723.31

Optional (These are not essential to autonomous flight navigation and surveillance)			
Tail Fin with Rudder	57.57	1	57.57
3.5m GPS Antenna Cable	51.82	1	51.82
RC Receiver	24.3	1	24.3
RC Motor Speed Controller	8.23	1	8.23
Subtotal			141.92

Appendix 8.9

Payloads and Weight Considerations of Different Sized Airships

Airship Size and Payload Considerations

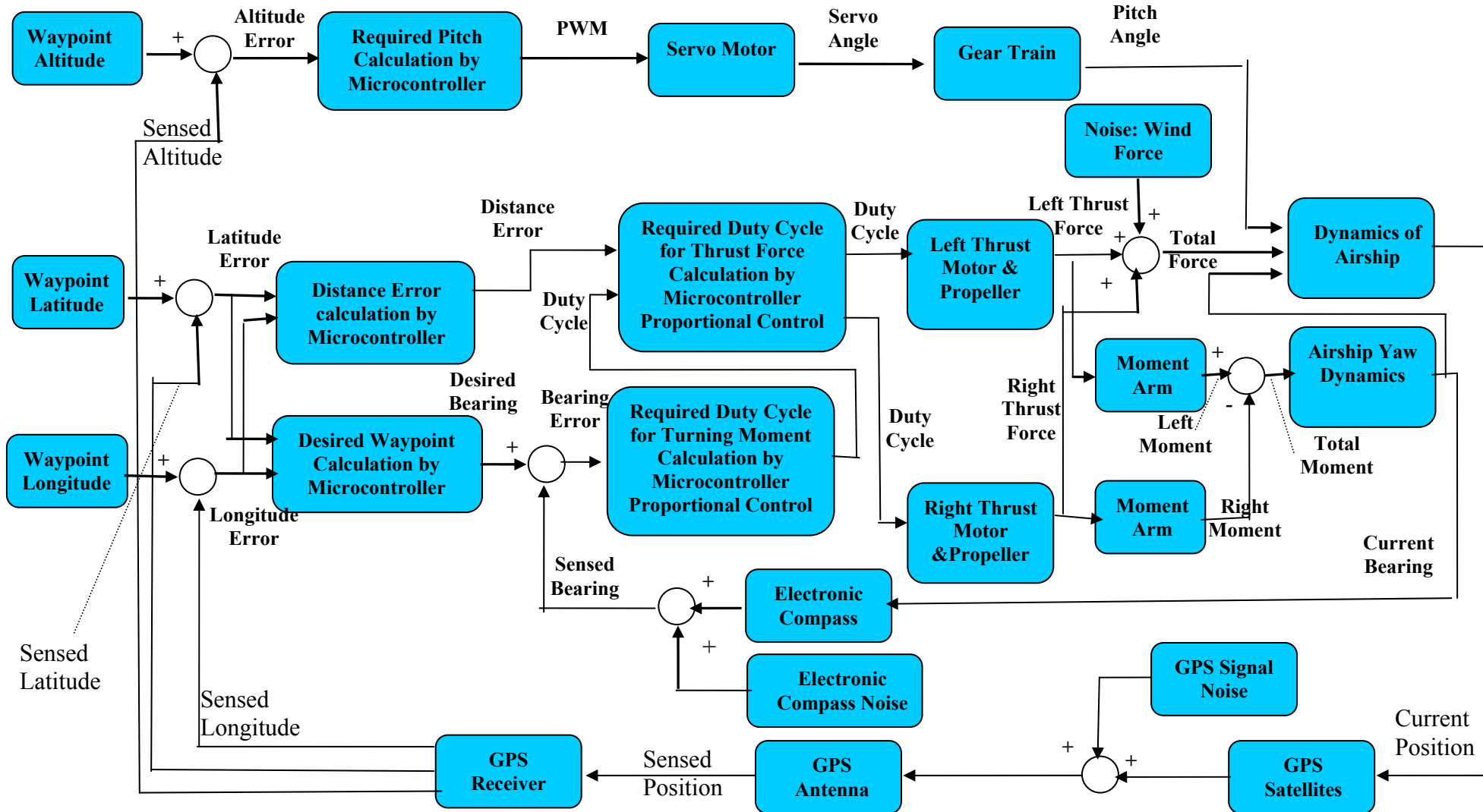
Airship Length / feet (m)	Airship Diameter/ inch (m)	Volume of Gas Envelope /m ³	Maximum Payload /kg	Weight of Fixed Components / kg	Weight allowed for Variable components / kg	Cost of Gas Bag (Singapore \$)*
7.0ft (2.1m)	32" (0.8128m)	1.1327	0.7988	0.561	0.2378	\$572.71
7.5ft (2.3m)	44" (1.1176m)	1.4158	0.9356	0.561	0.3746	\$648.20
8.0ft (2.4m)	47" (1.19380m)	1.8406	1.191	0.561	0.63	\$812.30
9.0ft (2.8m)	52" (1.3208m)	2.5485	1.701	0.561	1.14	\$1,066.65
10.0ft (3m)	58" (1.4732m)	3.6812	2.404	0.561	1.843	\$1,230.75
11.0 ft (3.4m)	63.6" (1.6154m)	3.9643	2.586	0.561	2.025	\$1,312.80
11.5ft (3.5m)	66" (1.6764m)	4.5307	2.767	0.561	2.206	\$1,394.85
13.0ft (4m)	69.6" (1.7678m)	6.5129	4.355	0.561	3.794	\$1,723.05

*Currency conversion rate is US\$1 = Singapore\$1.6410

** Information provided kindly by Mr. Dan Speers, Mobile Airships Inc

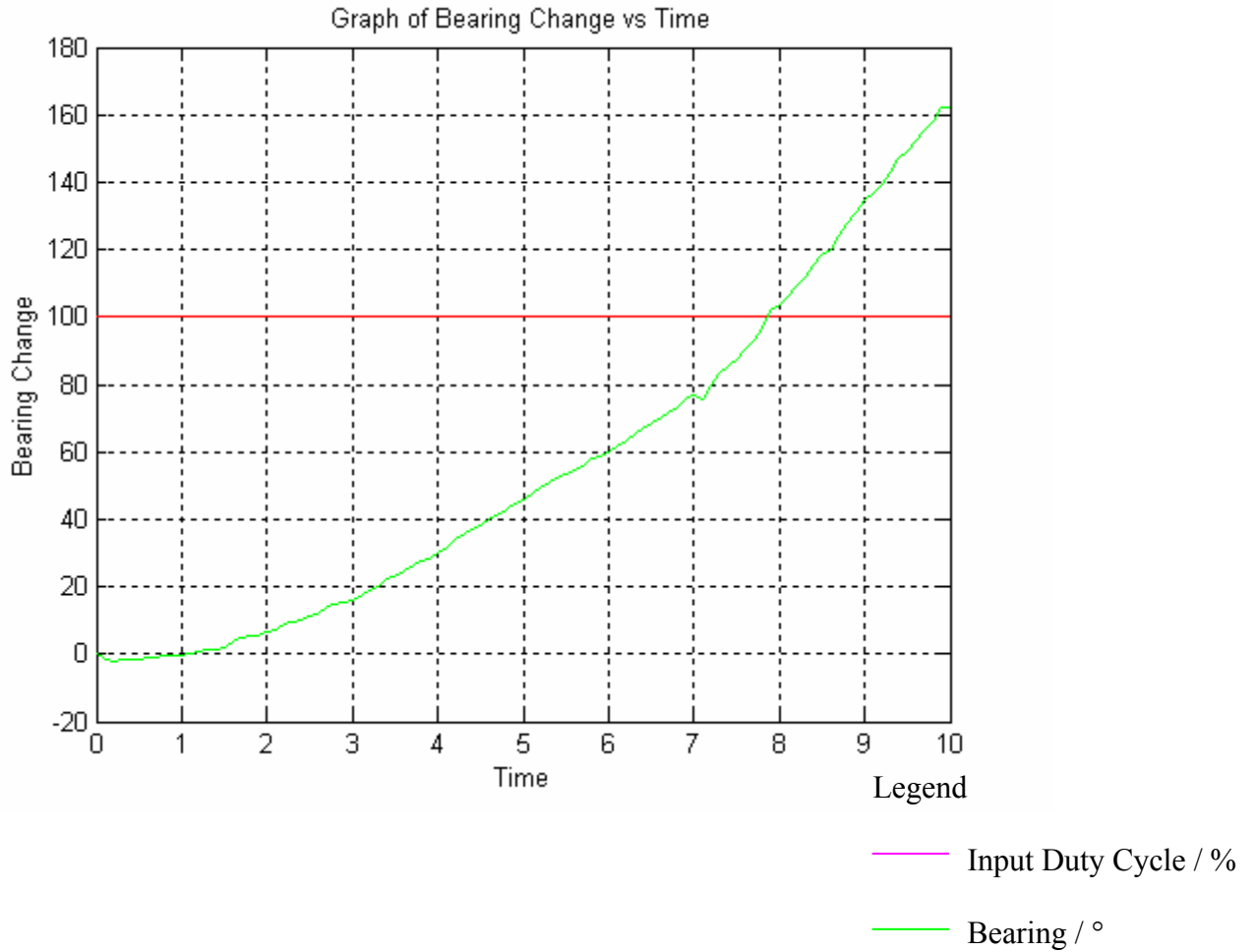
Appendix 9.1

Block Diagram of GPS Navigation Control Loop



Appendix 9.2

Output Response of Plant to Step Input

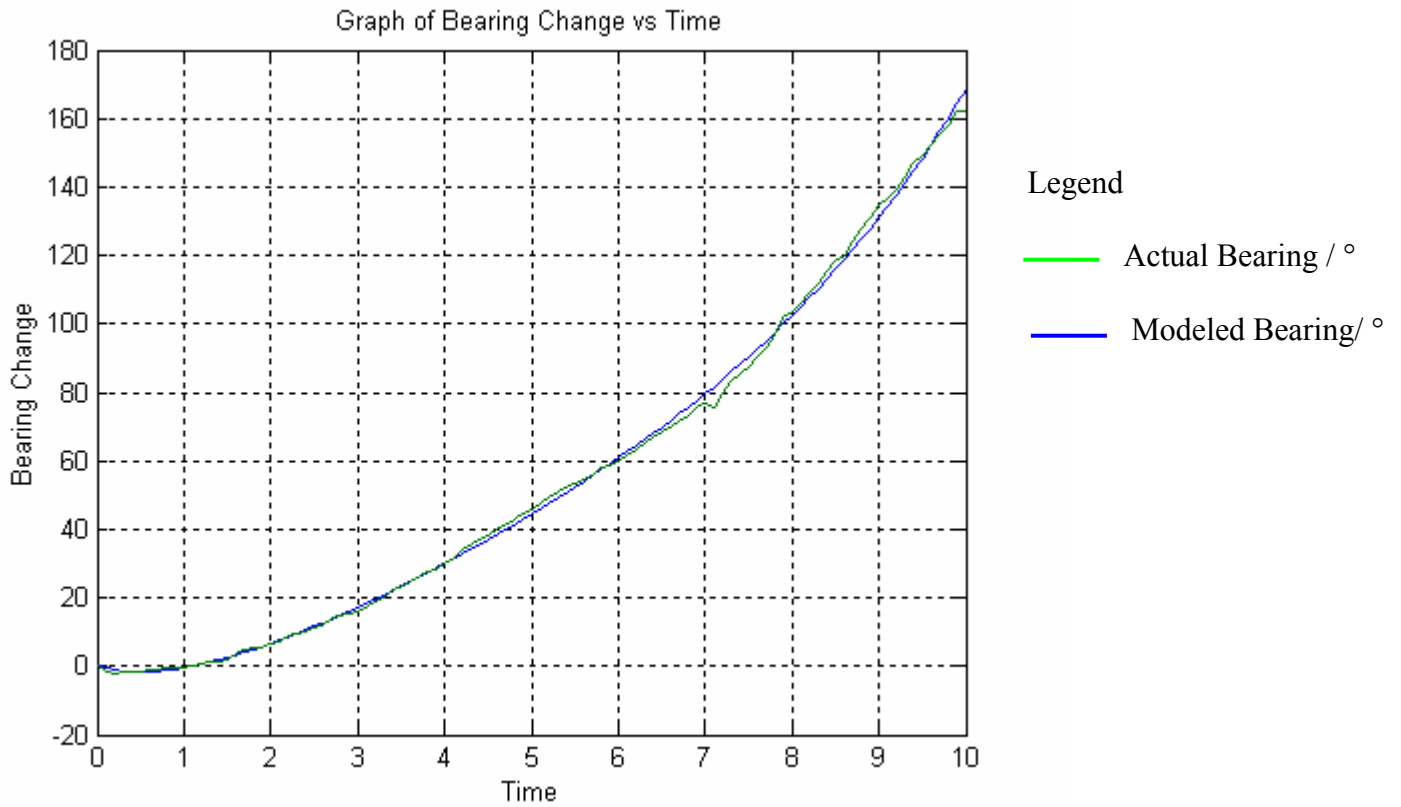


The input, $V(t)$, is a unit step voltage of duty cycle 100% at time $t=0$:

$$V(t) = 100u(t)$$

Appendix 9.3

Curve Fitting Using Complex RF



The equation of the curve is given by:

$$\theta(t) = 0.9283e^{0.4341t} + 7.4780e^{-0.1389t} + 18.1052e^{-0.8570t} + 4.8535e^{-0.5598t} + 12.6823t - 31.4568$$

30 Trials were done and the curve with the Minimum Error_{RMS} was used.

Trial Number	RMS Error of Curve Fitting
1	17.4198
2	77.618
3	17.5472
4	17.8593
5	17.6239
6	18.7148
7	22.9833
8	17.9167
9	17.574
10	77.6868
11	17.6979
12	17.7637
13	17.9114
14	17.9795
15	17.7961
16	18.2536
17	17.6034
18	17.7652
19	18.9586
20	17.8022
21	18.0241
22	77.7055
23	18.2504
24	17.4305
25	18.8719
26	77.6157
27	17.646
28	20.6867
29	17.6894
30	17.949

Appendix 9.4

Derivation of Transfer Function of Plant

$$V(t) = 100u(t)$$

$$V(s) = \frac{100}{s}$$

$$\theta(t) = 0.9283e^{0.4341t} + 7.4780e^{-0.1389t} + 18.1052e^{-0.8570t} + 4.8535e^{-0.5598t} + 12.6823t - 31.4568$$

$$\theta(s) = \frac{0.9283}{1-0.4341s} + \frac{7.478}{1+0.1389s} + \frac{18.1052}{1+0.8570s} + \frac{4.8535}{1+0.5598s} + \frac{12.6823}{s^2} - \frac{31.4568}{s}$$

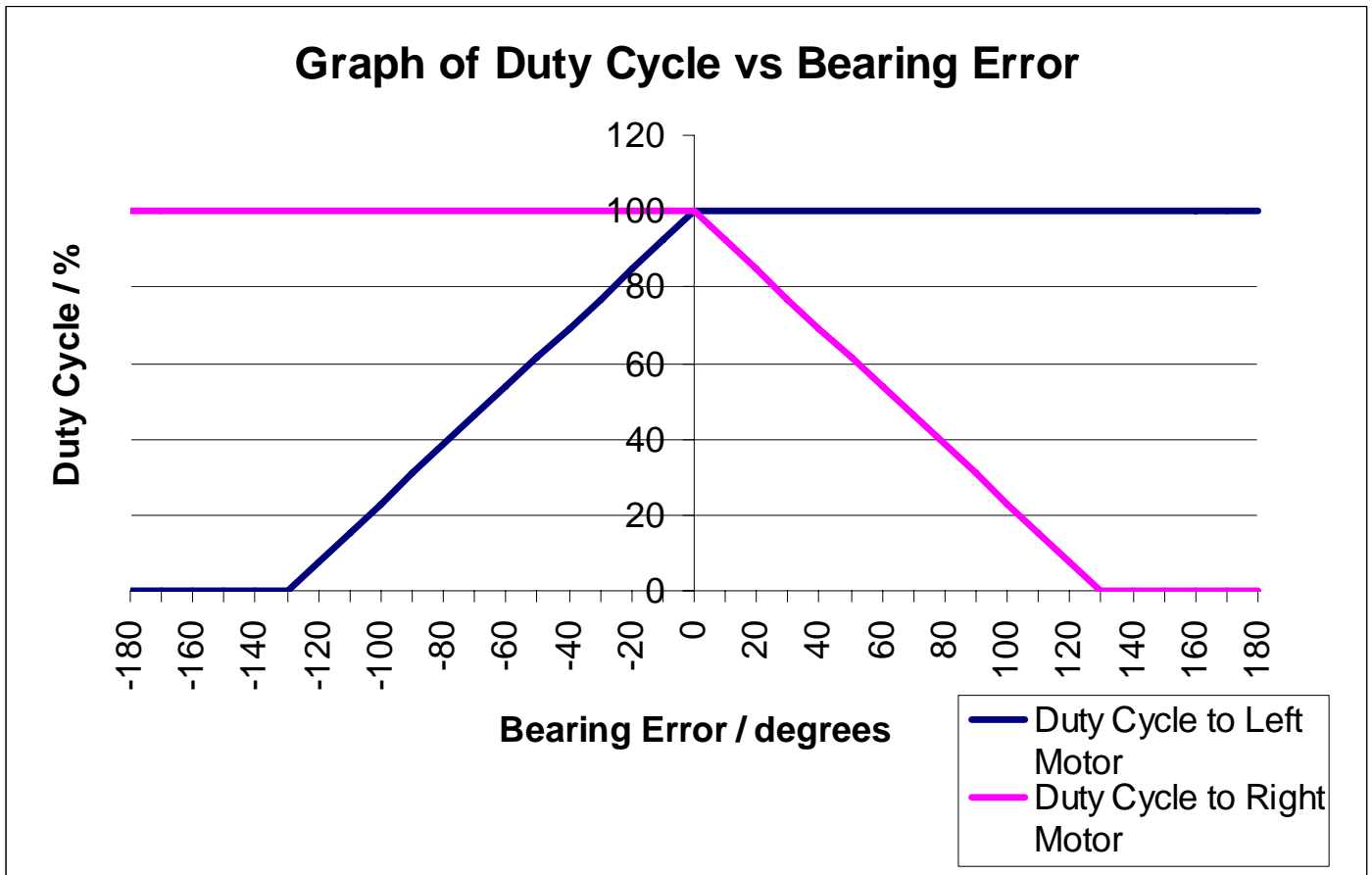
$$\theta(s) = \frac{12.6823s + 45.68127s^2 + 66.66233s^3 + 13.46875s^4 - 13.4969s^5 - 3.26738s^6}{s^3 + 1.1216s^4 + 0.001213s^5 - 0.22705s^6 - 0.02893s^7}$$

Therefore the transfer function $T(s)$ is given by:

$$T(s) = \frac{\theta(s)}{V(s)} = \frac{100 \times (12.6823s + 45.68127s^2 + 66.66233s^3 + 13.46875s^4 - 13.4969s^5 - 3.26738s^6)}{s^4 + 1.1216s^5 + 0.001213s^6 - 0.22705s^7 - 0.02893s^8}$$

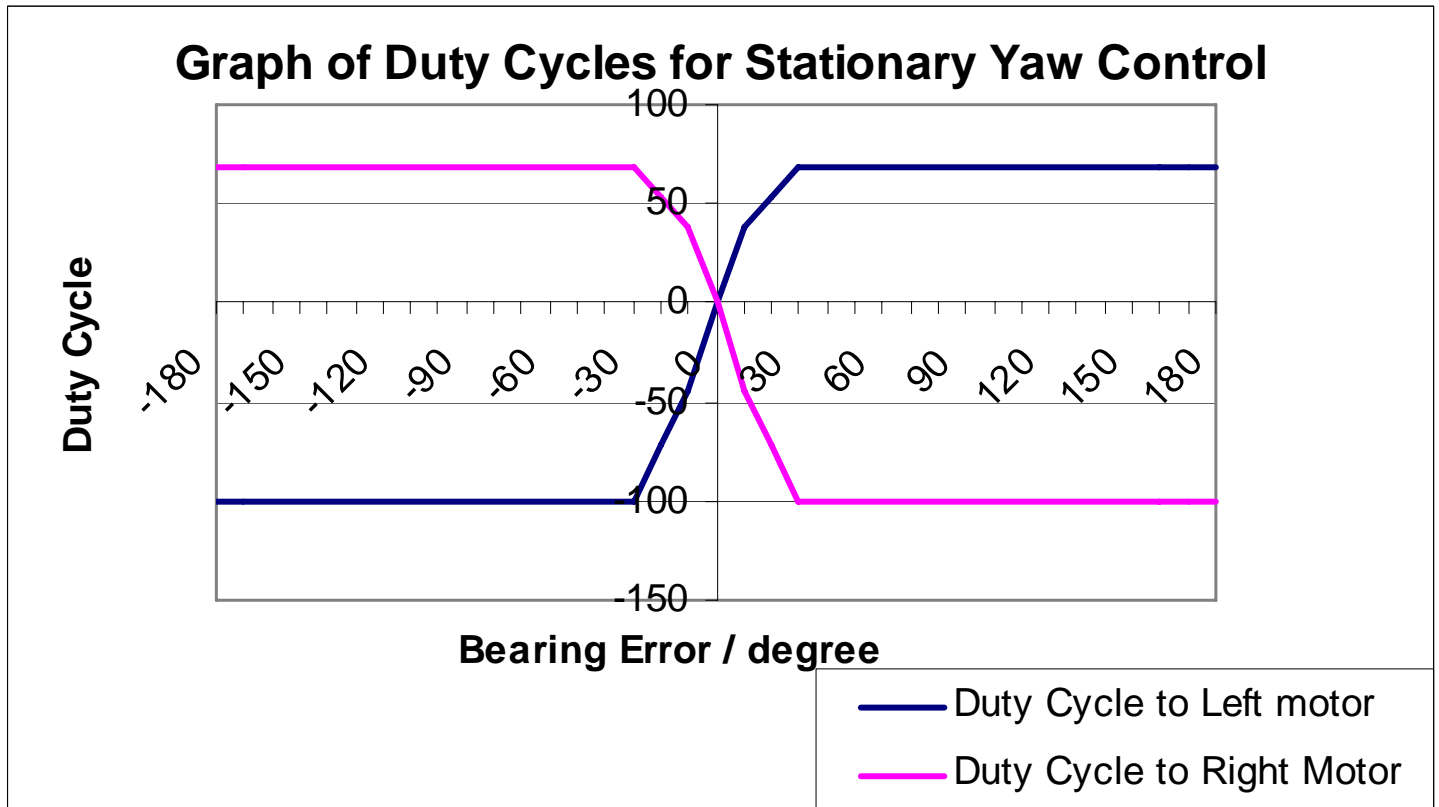
Appendix 9.5

Graph of Duty Cycle Vs Bearing Error for Navigational Yaw Control



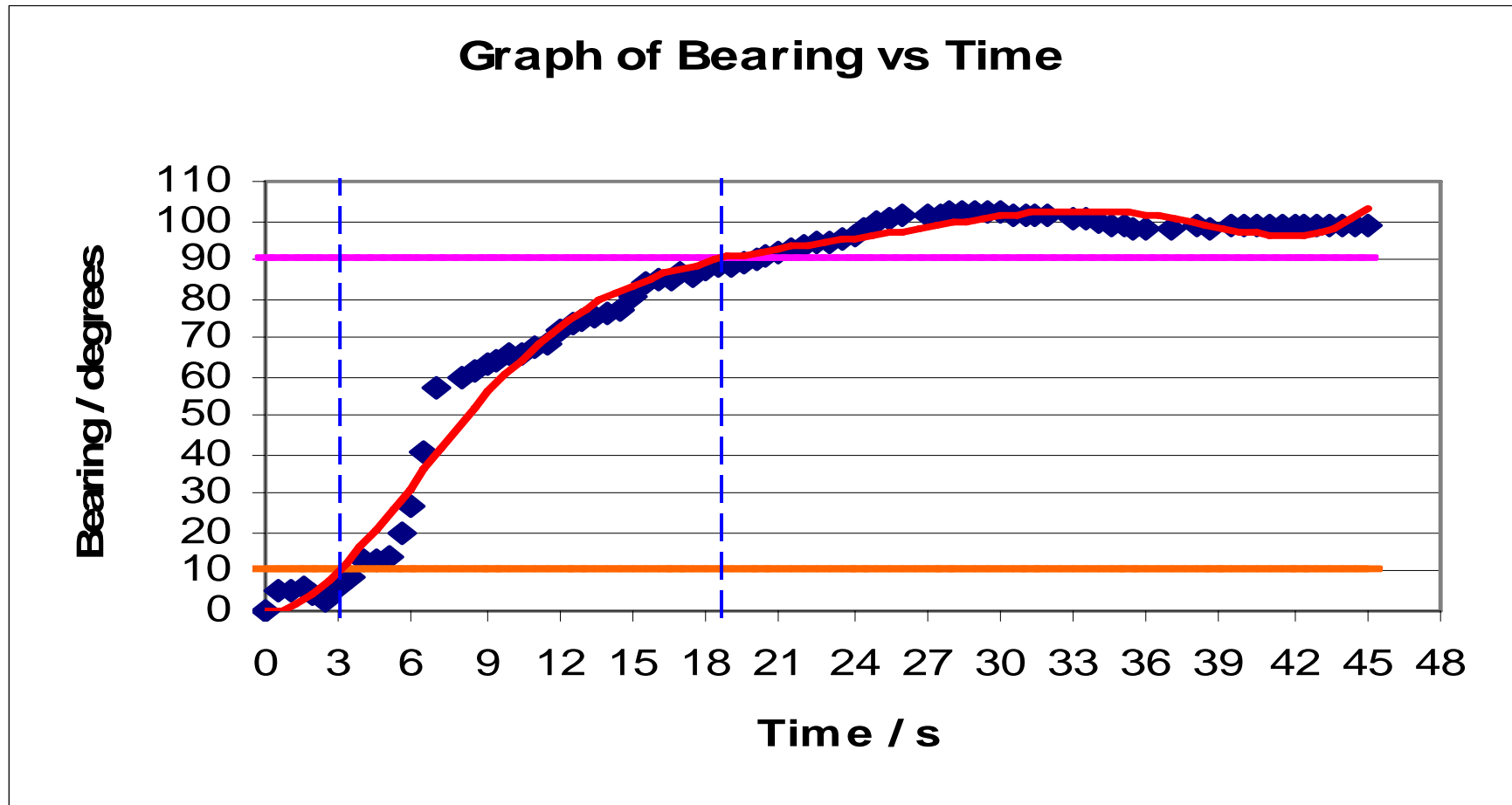
Appendix 9.6

Graph of Duty Cycle Vs Bearing Error for Stationary Yaw Control



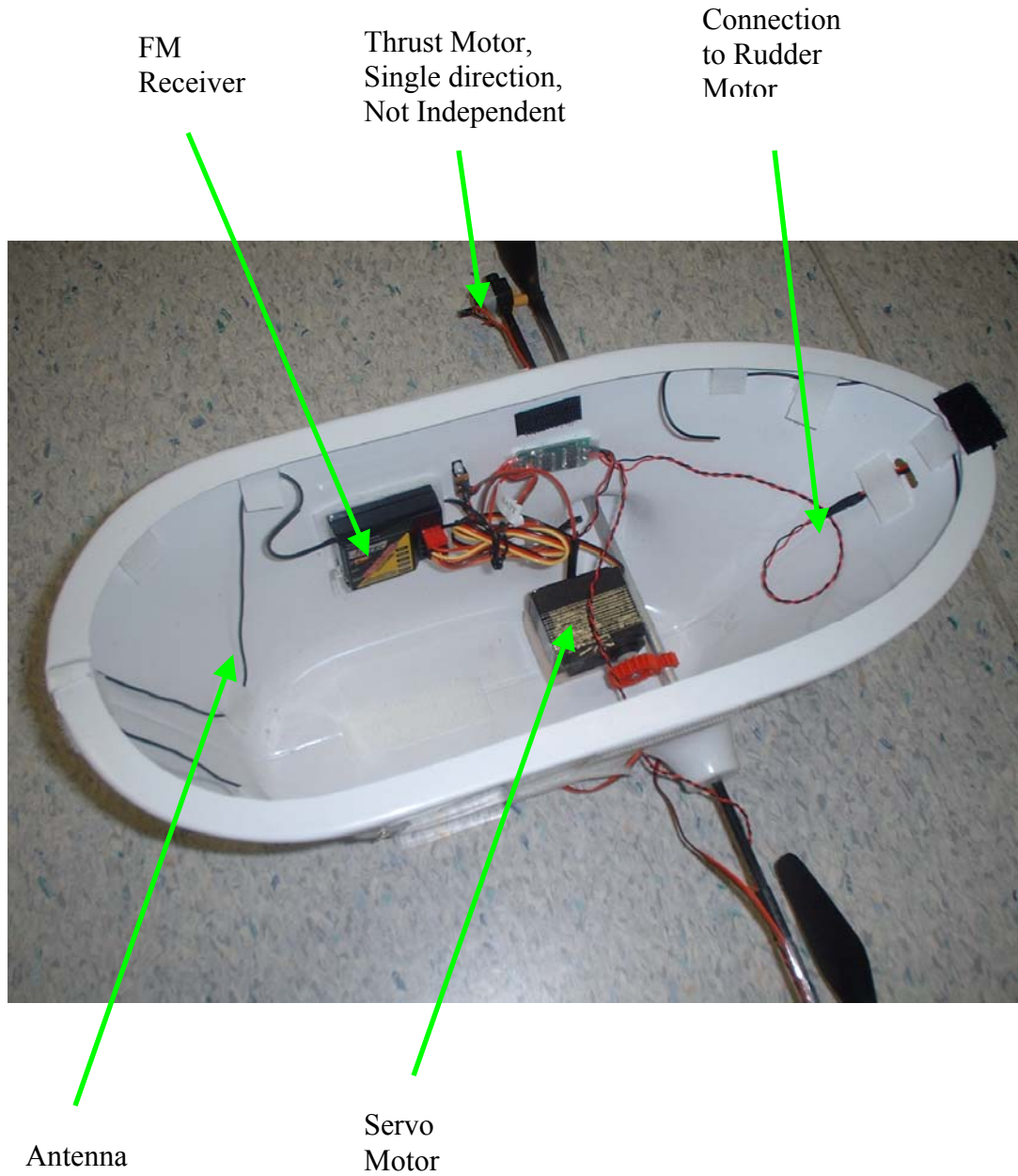
Appendix 9.7

Graph to Determine Rise Time



Appendix 10.1

Components in Unmodified Gondola



Appendix 10.2

Components in Modified Gondola

